Dhakshinamoorthy, A.; Asiri, AM.; García Gómez, H. (2017). Tuneable nature of metal organic frameworks as heterogeneous solid catalysts for alcohol oxidation. Chemical Communications. 53(79):10851-10869. doi:10.1039/c7cc05927b

Journal Name

ARTICLE

Tuneable Nature of Metal Organic Frameworks as Heterogeneous Solid Catalysts for Alcohol Oxidation

Amarajothi Dhakshinamoorthy,*[a] Abdullah M. Asiri,[c] Hermenegildo Garcia*[b,c]

Received 00th January 20xx,
Accepted 00th January 20xx

DOI: 10.1039/x0xx00000x

www.rsc.org/

Selective benzyl alcohol oxidation (BA) to benzaldehyde has been frequently used as a benchmark reaction to evaluate the catalytic activity of metal organic frameworks (MOFs) as oxidation catalysts. Substituted BAs, aliphatic and allylic alcohols have also been often used as substrates in these studies. In the present review, the current state of the art of MOFs as heterogeneous catalysts for BA and other alcohols oxidation is described, grouping the reports according to the nature of active sites present on MOFs. Thus, MOFs in which the catalytic centres are located at the ligands, at metallic nodes, at metal nanoparticles (MNPs) incorporated within the MOF pores or photoassisted oxidations have been commented. The aim of this review is to stress the current limitations encountered in the use of MOFs, particularly with respect to MOF stability and activity and propose new targets in the area.

1. Introduction

Metal organic frameworks (MOFs) have become among the currently most studied solids in heterogeneous catalysis.[1-6] The major reasons for this interest in applying MOFs as solid catalysts derive from the high percentage of transition metals, frequently with coordinative positions not compromised with the framework construction or having structural defects,[7, 8] the large surface area, high porosity and wide flexibility in the choice of transition metal and organic linkers.[9] MOFs are porous crystalline materials in where the lattice is maintained by coordinative ligand-metal interactions, very often involving also Coulombic attractions. In the MOF lattice, the nodes are constituted by metal ions or clusters of a few metal ions that may contain oxygen bridges coordinated with organic linkers having at least two binding positions in a rigid orientation.[10, 11] MOFs are among the porous solids with the largest empty space and lowest framework density having pore sizes in micro/meso dimension.[12]

The presence of metallic nodes in MOFs (Scheme 1) can promote a wide range of organic reactions, particularly for oxidations. Transition metal ions are among the most general oxidation catalysts, either as Lewis acids enhancing oxidant reactivity or by the reversible swing between two oxidation states of the metal.[13] Thus, oxygen activation can occur through direct electron transfer between O_2 and the metal ion in a high oxidation state, by coordination forming metal peroxides or can be even achieved by activation of aldehydes or radical initiators.[14]

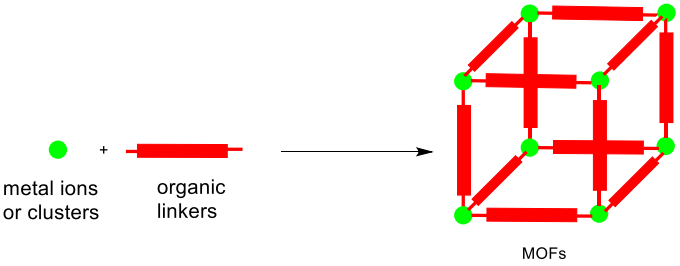

Scheme 1. A general structure of MOFs.

Due to the presence of organic components, MOFs are generally not suitable as catalysts for gas-phase reactions taking place at high temperatures,[15] however, there are many examples of MOFs whose structure is compatible with the conditions used in liquid phase reactions due to their milder conditions.[4, 16] MOFs have been reported to be active catalysts for a wide range of reactions including oxidations,[13, 17] cross-couplings,[5] condensations[18] and rearrangements,[19] among others. Particularly, due to the general activity of transition metals to promote oxidations, there is abundant literature about the use of MOFs as catalysts for oxidation of acyclic and cyclic hydrocarbons, benzylic positions and unsaturated multiple bonds.[13, 17, 20] One of the oxidation reactions that has higher importance in organic synthesis and has also industrial relevance is the oxidation of alcohols to carbonyl compounds,[21-24] there being much interest in developing a highly active MOF oxidation catalysts able to operate under mild conditions. In this context, the present Feature article is primarily focussed on the description of the state of the art on the use of MOFs for

[a] School of Chemistry, Madurai Kamaraj University, Tamil Nadu, India 625 021. E-mail: admguru@gmail.com
[b] Instituto Universitario de Tecnología Química CSIV-UPV, Universitat Politècnica de València, Av. De los Naranjos s/n, 46022, Valencia, Spain. E-mail: hgarcia@qim.upv.es
[c] Centre of Excellence for Advanced Materials Research, King Abdulaziz University, Jeddah, Saudi Arabia.

oxidation of BA, but also other aromatic and aliphatic alcohols. Besides the interest in organic synthesis and in the production of fine chemicals, the oxidation of BA is taken in the literature as model reaction to evaluate and to rank the catalytic activity of any new MOF material that can potentially be used as oxidation catalyst.

In the present feature article, we summarize those reports that have studied the catalytic activity of MOFs for the oxidation of BA, either using hydroperoxide, molecular oxygen, or other oxidizing reagent either thermally or under assistance of light. This review is organized by grouping the existing literature as a function of whether the active sites are at the organic linker, at the metal nodes or due to the presence of complex/metal nanoparticles (NPs) or other guest embedded at the pores. A specific section describes the photocatalytic activity of some MOFs to promote aerobic oxidation upon light irradiation. On the other hand, the active sites in MOFs can also be formed during the course of the reaction upon adsorption of the reactants.[25] For instance, the crystal structure of $Cu_3(BTC)_2$ consists of a pair of Cu^{2+} cations bridged by four carboxylate groups of four different BTC linkers in paddlewheel units. Furthermore, the Cu^{2+} ions remain coordinatively unsaturated with one vacant coordination positions at each Cu^{2+} ion that contributes to Lewis acidity. In addition, high concentration of Cu^{2+} in $Cu_3(BTC)_2$ results in relatively close proximity between Cu^{2+} cations which are separated only by 8.2 Å and are accessible through supercage. The close proximity of the active sites allows simultaneous interaction of larger molecules with multiple active sites (typically more than one Cu^{2+} cation). This two-site adsorption has significantly improved the catalytic activity of $Cu_3(BTC)_2$ in Friedlander reaction as evidenced by theoretical calculations.[26] In another example, the unusual high activity of $Cu_3(BTC)_2$ in Knoevenagel condensation of benzaldehyde with malononitrile was proposed to be due to three factors as supported by density functional calculation.[27] The first factor is that $Cu_3(BTC)_2$ can act as a base, and the active methylene group in malononitrile is deprotonated by creating a temporary defect in the framework. Then, this defect acts as a Brönsted acid site, activating simultaneously the aldehyde. The third factor is that malononitrile undergoes activation by two adjacent Cu^{2+} sites (Lewis acid sites) that are suitable located at the adequate distance to interact with each nitrile group of the reagent.

The purpose of this review is to clarify the field by indicating the most active materials reported so far and the reaction conditions that should be taken as benchmark to compare new MOFs and also to indicate some best practices to be followed in the evaluation of MOFs as oxidation catalysts for BA or alcohols in general. In this regard, one of the main points to be considered is catalyst stability under the reaction conditions. Since one of the main advantages of heterogeneous catalysts is reusability, catalyst stability has to be proved by providing time-conversion plots showing that the initial reaction rate and final yields are not altered upon catalyst recycle and also by complete chemical analysis of the liquid phase at final reaction time. These data have to be complemented by characterization of the used solid sample, determining their composition, particle size and morphology, crystallinity and porosity after consecutive uses of the same sample in comparison with the properties of the fresh material. It happens frequently in the literature that the stability of the MOF catalyst is claimed just by giving yields at final reaction times or some specific piece of information without a complete evaluation of the performance and properties of the solid material.[28] Although $Cu_3(BTC)_2$ exhibits unique activity compared to analogues MOFs in dehydrogenative coupling of silanes with alcohols[29] and in the synthesis of borasiloxanes by oxidative hydrolysis of silanes and pinacolborane,[30] it is reported to be unstable in the aerobic oxidation of thiols,[31] synthesis of 2-phenylquinoxaline[32] and reduction of acetophenone using silane as the reducing agent.[33] The reasons for deactivation or structural damage may be due to the ability of reactants to break the metal-ligand coordination bond. Therefore, care must be taken to select appropriate regents/reactants to preserve MOF stability under the reaction conditions.

In general, framework stability in MOF catalysis is assessed by performing leaching tests. One of the common methods for the determination of leaching of metal species (active sites) in heterogeneous catalysis is the so-called "*hot filtration*" test. This test is normally performed under the optimized reaction conditions, but the solid catalyst is filtered at the reaction temperature at a conversion of above 20 %. Then, the filtrate in the absence of solid catalyst is further allowed to progress under the optimized reaction conditions. No further conversion should be observed if catalytically relevant concentrations of leached metal species are not present in the liquid phase. Maintaining the reaction temperature during the filtration step is necessary to avoid precipitation of the leached metal species. To reach a significant substrate conversion before filtration in hot ensures that the products that could be responsible for the leaching are already formed.

If in the leaching experiment an increase of substrate conversion with decreased rate compared to optimized conditions is observed after solid removal, the data indicates a partial contribution of metal leaching to the overall catalytic process. Figure 1 illustrates two possible time-conversion plots that can be observed in the hot filtration test.

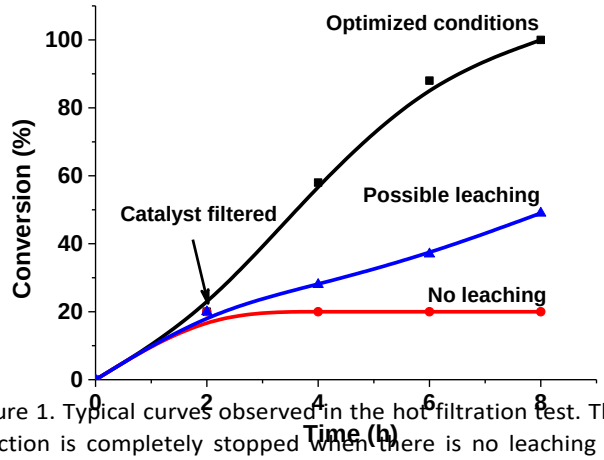

Figure 1. Typical curves observed in the hot filtration test. The reaction is completely stopped when there is no leaching of metal while there is a possible leaching if the reaction

continuous with decrease of rate in the absence of catalyst compared to optimized conditions.

One of the main reasons for selecting BA oxidation as a model reaction is the ease in which the reaction can be followed, together with the relevance of the process from the industrial point of view and also the ease of this particular oxidation when using BA as a probe molecule. Attention has to be paid to the reaction conditions employed including substrate/catalyst molar ratio, the reaction temperature, the nature of the solvent employed, the amount of the base used and the addition of co-catalyst. Obviously, the target is to use the minimum amount of metal, to perform the reaction at room temperature and in the absence of solvents or in the presence of environmentally benign liquid phases. One point to be considered is the nature and concentration of the base frequently required to promote oxidation. Generally, the role of the base in the reaction mechanism is to shift the alcohol/alcoholate dissociation equilibrium towards the alcoholate by abstracting a proton. The presence of a base increases the concentration of alcoholate that binds considerably stronger to the metal ions than the alcohol, thus favouring the oxidation mechanism. For example, the choice of a base has very strong influence in the catalytic activity as well as structural stability in Suzuki–Miyaura cross-coupling reaction using Pd@NH_2-MIL-101(Cr) as catalyst.[34] The use of carbonates (K_2CO_3 and Cs_2CO_3) as bases resulted in higher yields in short reaction times, but also leads to decomposition of the MOF. On the other hand, using fluorides (KF and CsF) as the base, required longer times to achieve higher activity, but, however, the crystallinity and porosity of the MOF are preserved under the reaction conditions tested here. However, since many MOFs are not stable in the presence of bases, and also from the point of view of the greenness of the process, it would be much more convenient to avoid/minimize the base concentration. It has to be remarked that as the MOF lattice is mainly based on metal-ligand coordination bonds, bases can disrupt this interaction by coordinating with the metal ions stronger than the ligand. In the absence of a base, alcohols, instead of alcoholates, have to bind to the metal cation. This interaction of alcohols are less strong than those of alcoholates due to the absence of negative charge and the lower electronic density of alcohols as base. Therefore, binding of alcohols rather than alcoholates requires of metal cations with stronger Lewis acidity.

Also, there are many examples in the literature describing a combination of dissolved transition metals with 2,2,6,6-tetramethylpiperidine 1-oxyl **(**TEMPO) as cocatalysts for the alcohol oxidation.[35-41] Analogously, there are several reports in which the catalytic activity of MOFs to promote aerobic oxidation has been assessed in the presence of cocatalysts, TEMPO, being among the preferred ones. Some of these systems are inspired by natural enzymes such as oxidases and oxygenases,[42] where the active prosthetic centre of the protein is constituted by metals surrounded amino acids that can generate oxyl radicals analogous to TEMPO. Obviously from the point of view of the catalytic activity, it would be desirable to avoid or to minimize as much as possible the presence of these added cocatalysts that have to be added in each consecutive use.

A final point to be considered is the scope of MOFs as catalysts in alcohol oxidation. Thus, besides BA, other benzylic compounds should also be screened including secondary benzyl alcohols. Secondary alcohols can react slower than primary alcohols when the steric hindrance around the hydroxyl group is controlling the reaction rate. However, secondary benzyl alcohols can be oxidized involving radicals and other reaction intermediates that are more stable, therefore formed with less activation energy, than analogue intermediates of the primary BAs and, therefore, they can react faster. Accordingly the relative reaction rates between primary and secondary benzyl alcohols can give certain information about the accessibility of active sites. Those active sites that are less accessible and are confined in a restricted space exhibit a general higher activity for primary alcohols due to their lower steric encumbrance. In this regard, the presence of active sites inside the pores can also lead to the observation of shape selectivity, where the higher reactivity of substrates or the product selectivity derives from the different geometry and dimension of the substrates and products. Also with respect to the scope, besides benzyl alcohols, other types of alcohols including alkyl and cycloalkyl, primary/secondary substrates should be evaluated besides BA to determine the applicability of a given MOF as oxidation catalyst. In general, the trend in oxidation of alcohols is that the reactivity of acyclic secondary alcohols is lower than that of benzylic ones and their oxidation requires generally harsher reaction conditions to occur, i.e. higher temperature and the presence of base. All these aspects, reaction scope and conditions, catalyst stability, turnover number and turnover frequency have to be considered when evaluating a certain MOF material as oxidation catalyst for the transformation of alcohols into carbonyl compounds.

Although there is a large number of MOFs, many of them lack of sufficient stability or the pore sizes are insufficiently large, their synthesis is difficult or other negative structural or physiochemical features that limit their application in catalysis. Therefore, from the consideration of the prerequisite wanted in a MOF for their use in catalysis, it comes that there are some preferred MOFs that are most frequently used as catalysts and, particularly, the most deeply investigated with regard to their activity to promote oxidation of BA and other alcohols. For this reason, the next paragraphs describe the structure of some of the most relevant MOFs for the present review.

One of these materials is chromium(III) terephthalate, MIL-101(Cr)[43] with the molecular formula of $Cr_3(F,OH)$-$(H_2O)_2O[(O_2C)$-C_6H_4-$(CO_2)]_3 \cdot nH_2O$ (n=25). MIL-101(Cr) was synthesised by Ferey's group by reaction between a Cr^{3+} solution and 1,4-benzenedicarboxylate (BDC) as a ligand. Isostructural MIL-101(Cr) can also be prepared with Fe^{3+} instead of Cr^{3+}. This MOF has two types of zeotypic mesoporous pores (Figure 2) with free diameters of ca. 29 and 34 Å, respectively, accessible through two microporous windows of ca.12 and 16 Å. MIL-101(Cr) possesses very high BET surface area of 4100 m^2/g. On the other hand, this MOF contains potential unsaturated chromium sites (up to 3 mmol/g) where solvent

molecules or water can be adsorbed. These unsaturated coordination positions can be used as Lewis acid sites in many organic transformations.

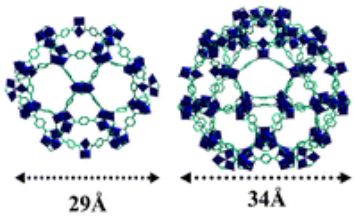

Figure 2. Illustration of the two types of cages present in the structure of MIL-101(Cr). Reproduced from ref. [44] with permission from the Royal Society of Chemistry.

Besides MIL-101(Cr or Fe), other preferred MOF as catalyst for alcohol oxidation is $Cu_3(BTC)_2$ (BTC: 1,3,5-benzenetricarboxylate), also known as HKUST-1 (Hong Kong University of Science and Technology) that has been one of the extensively studied three dimensional porous MOFs as catalyst. The structure of $Cu_3(BTC)_2$ is constructed by the coordination of Cu_2 units by four BTC groups through paddle-wheel like coordination mode (Figure 3).[45] $Cu_3(BTC)_2$ is stable up to 240 °C and, hence, it can be conveniently used as a solid catalyst for a wide range of liquid phase reactions.

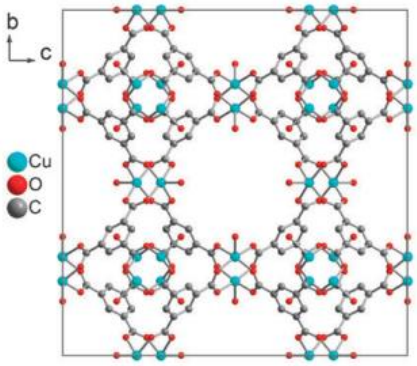

Figure 3. View of the packing of the cubic unit cell of $Cu_3(BTC)_2$ along the a axis to illustrate the analogy of this highly symmetric and porous framework with zeolites. Reproduced from ref. [45] with permission from the Science publishing group.

A third type of widely used MOF structure is UiO-66 (University of Oslo). It is obtained by the reaction of oxo zirconium salts with BDC, while its isostructural analogue, namely, UiO-67 is obtained similarly using 4,4'-biphenyldicarboxylate (BPDC) as linker (Figure 4). UiO type MOFs have been extensively used for many applications due to the fact that, particularly UiO-66, it is one of the most resistant MOFs in terms of both thermal and chemical stability.[46] On the other hand, several isostructural UiOs having substituents on the aromatic rings have been prepared due to the robustness of the framework[47] and hence, these MOFs allow the possibility to tune the acid strength at the $Zr_6(OH)_4O_4$ nodes or to introduce the basic sites within the framework by adequate substitution on the BDC linker.

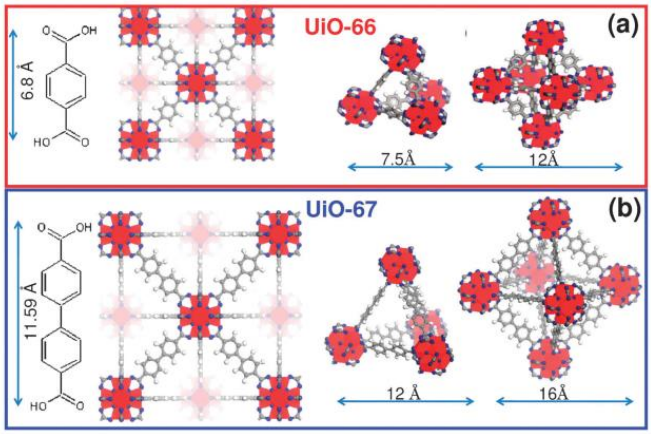

Figure 4. Structures of UiO-66 (a) and UiO-67 (b). Reproduced from ref. [48] with permission from Royal Society of Chemistry.

After having commented the structure of the three most used MOFs, Table 1 summarizes the reports that will be described below in the present review, indicating the corresponding MOF catalyst, the relevant reaction conditions and the resulting catalytic performance.

Table 1. List of MOFs that have been used as catalysts for alcohol oxidation.

Catalyst	Solvent, base, co-catalyst, oxidant	Conv.(%), Sel. (%), TON/(TOF)	Stability evidence	Ref.
Active sites at functionalized ligands				
Ru^{III}@MOF-253(Al)	CH_2Cl_2, -, -, $PhI(OAc)_2$	97, 100, (480 h^{-1})[b]	XRD, BET, leaching	[49]
$RuCl_3$@MIL-101(Cr)-TPY	H_2O, -, -, H_2O_2	99, 100, NR	Reuse, hot filtration	[50]
$Ir^{III}Cp^*Cl$@COMOC-4	Toluene, $CsCO_3$, -, O_2	54, 99, NR	XRD, reuse	[51]
UiO-66-CrCAT[a]	Chlorobenzene, -, -, TBHP	99, 100, (4.13 h^{-1})	Reuse, XRD, SEM	[52]
UiO-67-$FeCl_3$	CH_3CN, -, TEMPO and $NaNO_2$	99, 100, NR	XRD, IR, ICP-AES	[53]
UiO-66-Sal-$CuCl_2$	CH_3CN, $NaHCO_3$, TEMPO, O_2	99, 99, NR	XRD, IR	[54]
Cu(II)/MOF-NH_2	CH_3CN, -, TEMPO, air	99, 100, NR	XRD, FT-IR, XPS	[55]
CuI/MIL-101-N-2-PYC	CH_3CN, NMI, TEMPO, air	99, 100, NR	XRD, leaching	[56]
Cu(I)/UiO-66-NH-PC[b]	CH_3CN, NMI, TEMPO, air	99, 100, NR	XRD, SEM, reuse	[57]
Metal nodes as active centres				
$Pd(2\text{-}PYMO)_2$[c]	Toluene, -, -, air	99, 74, NR	-	[58]
$Cu_3(BTC)_2$	CH_3CN, Na_2CO_3, TEMPO, O_2	89, 100, 1.5	XRD	[59]
$Cu_3(BTC)_2$	CH_3CN, NMI, TEMPO, O_2	94, 100, NR	reuse	[60]

$Cu_3(BTC)_2$ different crystal size	CH_3CN, Na_2CO_3, TEMPO, O_2	100, 100, NR	reuse	61
Mesoporous $Cu_3(BTC)_2$	CH_3CN, -, TEMPO, O_2	100, 100, NR	XRD, leaching, reuse	62
SPS–Cu(II)@$Cu_3(BTC)_2$	CH_3CN, -, TEMPO, O_2	99, 100, NR	XRD, FESEM, reuse	63
Cu_2(BDDA)$(OAc)_2\cdot H_2O$	-, -, -, TBHP	95, 100, NR	Reuse, TEM	64
[{Cu(L1)(DMF)}·DMF·H_2O]$_n$	-, -, -, TBHP	81, 100, (811 h^{-1})	XRD	65
Cu-MOF-74	CH_3CN, DMAP, TEMPO, O_2	89, 100, NR	reuse	66
{[Cu_2(1,2-BDC)$_2$(FBTX)$_2$]·$3H_2O$}$_n$[d]	CH_3CN, Na_2CO_3, TEMPO, air	100, 100, NR	FT-IR, XRD, XPS, Reuse, leaching	67
$Co_3(BTC)_2$	DMF, -, -, O_2	92.9, 97, NR	XRD	68
Co(BDC)$(TED)_{0.5}$	DMF, -, -, O_2	81, 99, NR	Reuse, leaching	69
Co(L)(BDC)(MeOH)	CH_3CN, -, -, TBHP	88, 91, NR	XRD, reuse	70
STA-12(Co)[e]	Ethyl acetate, -, -, TBHP	50, 100, (9.6 h^{-1})[e]	XRD, reuse	71
Ce-UiO-66-BDC	CH_3CN, -, TEMPO, O_2	88, 100, NR	XRD	72
Photocatalytic oxidation				
NH_2-UiO-66-F	Toluene, -, -, O_2	53.9, 99, (410 µmol $min^{-1}g^{-1}$)	-	73
PCN-22	CH_3CN, -, TEMPO, O_2	28, 100, 100	reuse	74
70Ti@SHK2[f]	CH_3CN, -, -, O_2	89, 93, NR	reuse	75
MNPs@MOFs as active sites				
Pt@MOF-177 (Pt size: 2-5 nm)	-, -, -, O_2	50, 100, 968	XRD, reuse	76
Au/MIL-101(Cr) (Au size: 2.3 nm)	Toluene, -, -, O_2	100, 100, (29300 h^{-1})[b]	TEM, leaching	77
Au/PMA-MIL-101 (Au size: 2.5 nm)	Toluene, K_2CO_3, -, O_2	60, 100 (7 min^{-1})	reuse	78
Pd/MIL-101[c] (Pd size: 2.5±0.5 nm)	Toluene, -, -, O_2	99, 99 (16900 h^{-1})	XRD, AAS, reuse	79
Pd@Cu(II)-MOF (Pd size: 2 nm)	Xylene, -, -, O_2	95, 99, 19	HRTEM, Reuse, leaching	80

[a]oxidation of 2-heptanol; [b]Oxidation of 1-phenylethanol; [c]Oxidation of cinnamyl alcohol; [d]Oxidation of 4-methoxybenzyl alcohol; [e]4-chlorobenzyl alcohol; [f]4-methylbenzyl alcohol; Value in parenthesis represent TOF; NR stands for not reported; TPY: 2,2':6',2''-terpyridine; COMOC-4: nanoporous Ga-based MOF, Ga(OH)(BPYDC); BPYDC: 2,2'-bipyridine-5,5'-dicarboxylate; Cp*: 1,2,3,4,5-pentamethylcyclopentadienyl; TBHP: *t*-butylhydroperoxide; NMI: N-methylimidazole; PYC: pyridinecarbaldehde; 2-PYMO: 2-pyrimidinolate; BDDA: 4,4'-[benzene-1,4-diylbis (methylylidenenitrilo)] dibenzoic acid; DMAP: 4-dimethylaminopyridine; SPS: sulfonated-polystyrene; BTC: 1,3,5-benzenetricarboxylate; BDC:1,2-benzenedicarboxylate, FBTX: 1,4-bis(1,2,4-triazole-1-ylmethyl)-2,3,5,6-tetrafluorobenzene); TED: triethylenediamine; STA: St. Andrews porous material; PCN: porous coordination network; MOF-177: $[Zn_4O(BTB)_2]_8$; BTB: 1,3,5-benzenetribenzoic acid; PMA: phenylene-mono(oxamate); MOF-177: $[Zn_4O(BTB)_2]_8$; BTB:1,3,5-benzenetribenzoic acid.

After having listed the reports dealing with BA oxidation by MOFs, the following sections will focus on those reports in which the active sites are located either at the ligands, at the metal nodes or they are encapsulated as metal NPs within MOFs. A subsequent section will deal with photocatalytic BA oxidation promoted by MOFs.

2. Active sites at functionalized ligands

This section refers to examples of transition metal complexes attached to the linker as heterogeneous catalysts for oxidation of BA and other alcohols. Metal complexes are among the most general oxidation catalyst and in this section they have been attached to the linker in satellite positions. Thus, a ruthenium trichloride complex has been incorporated into the Al^{3+}-based MOF-253 having 2,2'-bpyridine ligands by post-synthetic modification to give Ru^{III}@MOF-253(Al) that presumably should have Ru-2,2'-bipyridyl complexes attached to the MOF-253(Al) lattice (Figure 5).[49] This MOF showed high catalytic activity for the oxidation of BA (TOF = 66 h^{-1}) or 1-phenylethanol (TOF = 97 h^{-1}) with $PhI(OAc)_2$ as oxidant at 40 °C. Ru^{III}@MOF-253(Al) was reused six times with only a moderate decrease in conversion of 1-phenylethanol. Interestingly, this catalyst afforded 89 % yield of cholestanone by oxidation of cholestanol (Scheme 2) under the optimized reaction conditions. However, oxidation of primary aliphatic alcohols, such as 1-nonanol or 2,2-dimethylpropan-1-ol, resulted in only traces of the corresponding aldehydes.

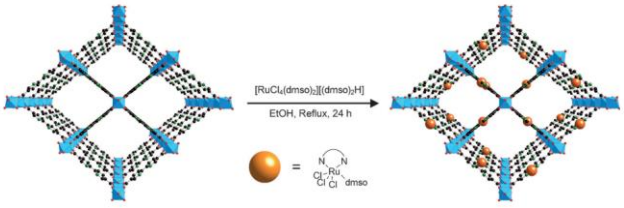

Figure 5. Illustration of the structure of MOF-253 showing the monodirectional topology with rectangular channels and its post-synthetic modification by forming a Ru-bipyridyl complex. Reproduced from ref. [49] with permission from Wiley.

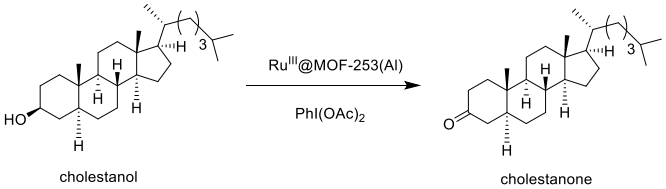

Scheme 2. Oxidation of cholestanol to cholestanone catalyzed by Ru^{III}@MOF-253(Al).

Synthesis of a tridentate oligopyridine σ-donor chelator (TPY, see structure in Figure 6), onto a new azide-tagged MIL-101(Cr)-N_3 has been achieved through a post-synthetic reaction after the preparation of the MOF based on the click cycloaddition. Later, $RuCl_3$ was added to form the corresponding complex on the tridentate chelator affording $RuCl_3$@MIL-101(Cr)-TPY catalyst.[50] This catalyst exhibited 99 % yield of benzaldehyde in the oxidation of BA at 100 °C using hydrogen peroxide as oxidant in water after 6 h. In contrast, the activity of $RuCl_3.3H_2O$ as a control showed only 49 % conversion of BA under identical conditions, although this model in the absence of TPY is different to the possible metal complexes encountered at $RuCl_3$@MIL-101(Cr)-TPY and other comparisons could be more appropriate to draw conclusions about the effect of MOF incorporation. The catalyst maintained its activity for five cycles without much significant loss of activity. Heterogeneity of the reaction was confirmed by a hot filtration experiment. It would have been of interest to check the activity of this catalyst for oxidation of primary and secondary aliphatic alcohols that are more challenging substrates.

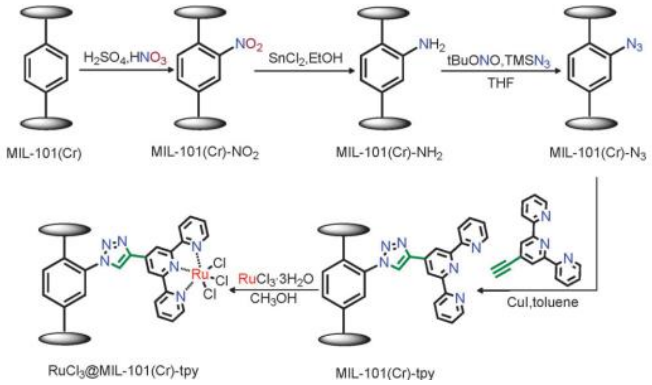

Figure 6. Post-synthesis modification of MIL-101(Cr) to synthesise a single-site heterogeneous Ru(III)-TPY catalyst. Reproduced from ref. [50] with permission from Royal Society of Chemistry.

Heterogenization of an Ir^{III} complex have been accomplished also through a 2,2'-bipyridyl unit by the modification of a nanoporous Ga-based Ga(OH)(BPYDC), denoted as COMOC-4.[51] Two different strategies, namely, post- and pre-synthetic functionalization (Figure 7) were followed to encapsulate Ir complex. It was found that the most convenient one was pre-synthetic functionalization, since it allowed a high Ir loading (0.67 $mmolg^{-1}$), while maintaining a large surface area (767 m^2/g) and still allowing the formation of the desired MOF structure. The Ir^{III}Cp*Cl@COMOC-4 material exhibited 54 % conversion of BA using Cs_2CO_3 as base with oxygen as oxidant at 150 °C after 24 h. Furthermore, no decrease in activity and selectivity was observed for Ir^{III}Cp*Cl@COMOC-4 catalyst in four cycles and powder XRD indicated that the crystalline structure is retained during the recycling experiments. Also, no significant leaching of the Ir and Ga species was observed. However, this catalyst suffers from serious limitations, like unsatisfactory 54 % conversion of BA and narrow substrate scope.

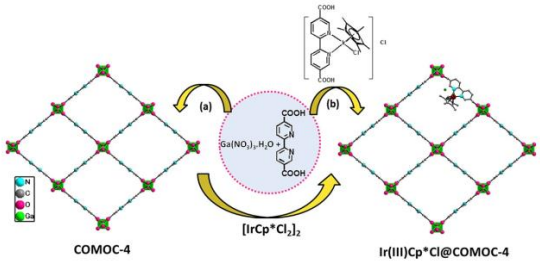

Figure 7. Illustration of the preparation of Ir^{III}Cp*Cl@COMOC-4 by a) post-synthetic or b) pre-synthetic functionalization. Reproduced from ref. [51] with permission from Wiley.

A new strategy has been reported to obtain metal-monocatecholato moieties in UiO-66 by two different post-synthetic strategies, namely, post-synthetic deprotection (PSD) and post-synthetic exchange (PSE).[52] Compared with PSD, PSE was found to be a more convenient and efficient approach to access efficient UiO-66 catalyst that could not be obtained directly in the solvothermal synthesis of the UiO-66. Furthermore, metalation of the catechol functionality attached to the MOF lattice resulted in UiO-66-CrCAT (Figure 8). The use of UiO-66-CrCAT (only 1 mol % Cr) afforded quantitative oxidation of 2-heptanol to 2-heptanone using TBHP as oxidant in chlorobenzene at 70 °C. On the other hand, a significant enhancement in the reaction rate was achieved with quantitative yield using only 0.5 mol % Cr loading under solvent-free conditions that are more attractive from the environmental point of view due to the avoidance of chlorinated solvents. Furthermore, unfunctionalized UiO-66 and UiO-66-CAT (via PSE without metalation) gave 8% and 12% yield of 2-heptanone at the same reaction time, respectively, showing the advantages of having the Cr-CAT complex. In addition, a series of aromatic, aliphatic and cyclic secondary alcohols were converted to their respective ketones in high yields both in chlorobenzene and under solvent-free conditions. Hot filtration experiment revealed the absence of catalytically active species in the solution (<0.1 ppm of Cr). The catalyst was reused for five consecutive runs without decrease in the yield at final reaction time. Characterization of UiO-66-CrCAT after catalysis showed the existence of high crystallinity as evidenced by powder XRD and SEM. Also, XPS and EXAFS analysis indicated after one-cycle of 2-heptanol oxidation no noticeable change in the coordination environment of the Cr centres, suggesting again that the catalytically relevant species is highly robust.

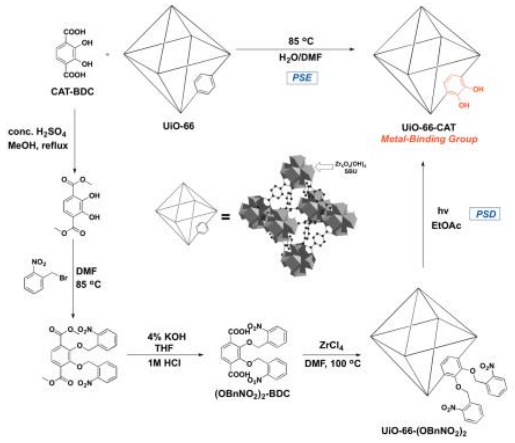

Figure 8. Synthesis of UiO-66-CAT via PSD or PSE. Reproduced from ref. [52] with permission from the American Chemical Society.

The use of TEMPO as co-catalyst in combination with soluble transition metal complex, particularly Cu^{II} but also Fe^{III}, allows to carry out oxidation of BA and other alcohols using molecular oxygen as terminal oxidizing reagent. The bipyridine units in UiO-67 were utilized for the immobilization of catalytically active iron species ($FeCl_3$) via a post-synthetic metalation method (Scheme 3) and the catalytic activity of the resulting MOF (UiO-67-$FeCl_3$) was examined in the oxidation of BA.[53] UiO-67-$FeCl_3$ afforded 99 % conversion of BA in combination with 10 mol% of $NaNO_2$ and 20 mol% of TEMPO in acetonitrile under aerobic conditions at room temperature. Under identical conditions, 1-phenylethanol and α-tetranol showed 63 and 52 % yields, respectively, but, however, no aliphatic alcohols were tested. The recovered UiO-67-$FeCl_3$ catalyst retained its efficiency and selectivity after five reaction cycles each of them requiring the continued addition of TEMPO. ICP-AES analysis of the filtrate gave an iron content of 6.3 ppm, corresponding to a minute amount of the total Fe content of the fresh catalyst. Powder XRD pattern and FT-IR spectra showed no significant differences between fresh UiO-67-$FeCl_3$ catalyst and five cycles recycled catalyst.

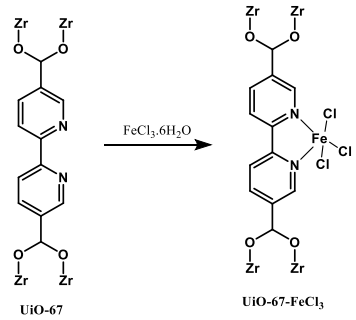

Scheme 3. Synthesis of UiO-67-$FeCl_3$ by post-synthetic modification of UiO-67 with $FeCl_3$.

A Zr-based UiO-66-NH_2 was functionalized with salicylaldehyde using a post-synthetic strategy to attach various copper (II) salts (Figure 9) and their activity was tested in the oxidation of BA.[54] For instance, UiO-66-Sal-Cu$(NO_3)_2$ catalyst showed 83 % conversion of BA with 99 % selectivity of the aldehyde under aerobic conditions using $NaHCO_3$ as base in acetonitrile with 0.25 mmol of TEMPO at 60 °C under oxygen atmosphere. On the other hand, UiO-66-Sal-Cu$(OAc)_2$ catalyst resulted in 68 % conversion with 99 % selectivity under identical conditions. Furthermore, UiO-66-Sal-$CuCl_2$ catalyst afforded 99 % conversion and selectivity under identical conditions. UiO-66-Sal-Cu$(OAc)_2$ showed 45 % conversion of 1-phenylethanol with 99 % selectivity of acetophenone under similar conditions. There was no leaching of copper during the reaction. The catalyst retained its activity even after five cycles, but TEMPO should be added each run. The powder XRD pattern and FTIR spectrum of five times recycled UiO-66-Sal-$CuCl_2$ catalyst was identical to that of the fresh catalyst, suggesting the structure and composition of UiO-66-NH_2 was largely retained.

Figure 9. Synthesis of UiO-66-Sal-$CuCl_2$. Reproduced from ref. [54] with permission from Elsevier.

Azide functionalized MOF, namely, MOF-N_3 was prepared following reported procedure,[81] and then, submitted to reduction to form the corresponding amine-functionalized MOFs.[82] This amine functionalized MOF was treated with $CuCl_2$ to obtain Cu(II)/MOF-NH_2 composite (Figure 10) and its activity in the oxidation of BA in the presence of TEMPO evaluated.[55] Under the optimized reaction conditions, Cu(II)/MOF-NH_2 and TEMPO as co-catalyst afforded in acetonitrile under air atmosphere at 70 °C complete BA conversion. In contrast, MOF-N_3 and MOF-NH_2 gave no conversion of BA, which confirmed that the oxidation of BA to benzaldehyde is catalysed by Cu. In addition, the use of $CuCl_2$ or a mixture of MOF-NH_2 and $CuCl_2$ showed 35 and 48 % yields, respectively, that are much lower than that of Cu(II)/MOF-NH_2-TEMPO. The enhanced activity of Cu(II)/MOF-NH_2 under base free conditions can be rationalized assuming that Cu(II)/MOF-NH_2 is acting not only as a catalyst but also as a base having much higher tendency to coordinate to Cu(II) to form the active species. A series of substituted BAs were converted to their respective aldehydes in moderate to high yields under identical conditions. Interestingly, 1-phenylethanol could also be oxidized to acetophenone with 98% yield. This catalyst was found to be heterogeneous in nature, but mediated by TEMPO in the liquid phase. The catalyst was reused for five runs with no appreciable change in the yield. Furthermore, XRD, FTIR and XP spectra of Cu(II)/MOF-NH_2 after five times recycling were identical to those of the fresh catalyst, suggesting that the structure is retained during the course of reaction.

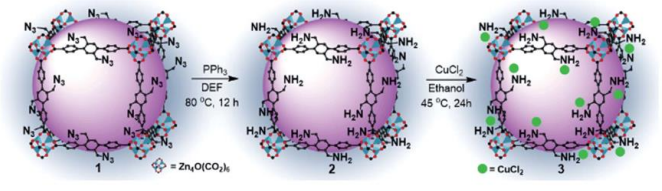

Figure 10. Post-functionalization route of the Cu(II)/MOF-NH_2 composite. Reproduced from ref. [55] with permission from Royal Society of Chemistry.

Recently, a newly designed iminopyridine derived MIL-101-N-2-PYC material was utilized for in situ complexation with copper(I) ion from CuI to form the CuI/MIL-101-N-2-PYC catalyst (Scheme 4).[56] The activity of this catalyst was examined in the oxidation of 1-phenylethanol using air as oxidant with 5 mol% TEMPO and 10 mol% NMI. Among the various catalysts tested for the oxidation of 1-phenylethanol, CuI/MIL-101-N-2-PYC showed 95 % yield in air at room temperature. Furthermore, CuI/MIL-101-N-2-PYC was used for the oxidation of BA to benzaldehyde with 99% yield under identical conditions. The catalyst was recycled for five times without any decay in its yield. The strong covalent bond between the iminopyridine moiety and the aromatic group ensures stability to the ligand during the reaction, since, otherwise imino groups are not stable and undergo fast hydrolysis to amino and aldehydes. A hot filtration test confirmed the absence of Cu leaching. Powder XRD pattern of the MIL-101-N-2-PYC after five catalytic cycles showed that the structure remained intact under the reaction conditions.

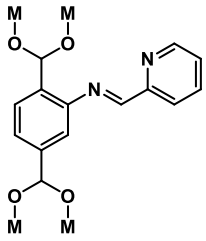

Scheme 4. Structure of MIL-101-N-2-PYC prepared by post-synthetic reaction of MIL-101-NH_2(Cr) and 2-pyridinecarbaldehyde.

Later, the same group has further reported pyridine-containing UiO-66-NH-PC material by peptide bond between UiO-66-NH_2 and a 2-pyridinecarboxylic acid chloride. The resulting pyridine-containing UiO-66-NH-PC was used to attach copper(I) salt to generate a Cu(I)/UiO-66-NH-PC complex (Figure 11). The activity of this complex was evaluated for 1-phenylethanol oxidation.[57] Among the various ligands examined for this reaction, this pyridine-derived MOF ligand showed the highest yield under the optimized reaction conditions. For example, a quantitative yield of acetophenone was observed with Cu(I)/UiO-66-NH-PC complex with 5 mol% TEMPO and 10 mol% NMI using air as oxidant at room temperature in acetonitrile. A series of secondary alcohols were also converted to their respective ketones in moderate to high yields under the optimized reaction conditions. Interestingly, this catalyst afforded 91 % yield of 2-adamantanone under the optimized reaction conditions. The catalyst was reused for five cycles with no decay in its activity using TEMPO and NMI in each run. There was no leaching of the active sites into the solution. In addition, the SEM image and XRD pattern of the fresh UiO-66-NH-PC ligand did not show any difference compared with five cycles used catalyst.

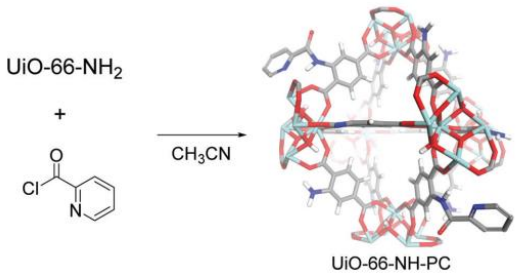

Figure 11. Synthesis of the UiO-66-NH-PC ligand with a post-synthetic modification. Reproduced from ref. [57] with permission from Royal Society of Chemistry.

Therefore, the current state of the art indicates that metal complexes bound to the MOF lattice at satellite positions can oxidize BA by air or molecular oxygen, but, then, homogeneous co-catalysts like TEMPO or the combination of TEMPO and NMI is needed. In this regard, the catalytic activity of the MIL-101 and UiO-66 containing Cu(I) is remarkable and appears general. It would be important to develop a MOF catalyst based on abundant metals that in the absence of any co-catalyst in the homogeneous phase is able to promote the room temperature oxidation of BA and other alcohols by air. One simple way, worth to be explored, is co-immobilization of co-catalyst also in the MOF structure, but this approach would require high cost in material preparation.

3. Metal nodes as active centres

In one of the earliest precedents, Pd(2-PYMO)$_2$ was reported as a solid catalyst for the oxidation of cinnamyl alcohol reaching complete conversion and 74 % selectivity to cinnamaldehyde using air at atmospheric pressure.[58] However, the stability of this Pd-containing MOF was not revealed, as well as the substrate scope beyond allylic alcohols. In any case, the use of cinnamyl alcohol as substrate is interesting because it allows to discriminate the selectivity for alcohol oxidation from other processes undergone at C=C bonds related to C=C oxidation or to the formation of metal hydride, including C=C reduction and allylic alcohol isomerization, among others.

Copper MOFs are the most widely used MOFs for BA and alcohol oxidation, due to the intrinsic activity of this transition metal as oxidizing catalyst. One of the most widely available, easy to prepare Cu MOFs is $Cu_3(BTC)_2$ whose structure has been already presented in a previous section. A series of articles have reported the catalytic activity of this $Cu_3(BTC)_2$ for aerobic oxidations of BA in the presence of TEMPO as co-catalyst. In several of these reports the size, porosity or arrangement of the $Cu_3(BTC)_2$ crystallites have been controlled and modified to evaluate the activity or stability of this MOF. In the first of these articles, aerobic oxidation of BA was reported in acetonitrile at 75 ^oC with $Cu_3(BTC)_2$ as catalyst, but required the presence of Na_2CO_3 and catalytic amounts of TEMPO to afford 89 % benzaldehyde yield.[59] Unfortunately, powder XRD analysis of the recovered catalyst revealed significant changes in its crystal structure compared with the fresh catalyst, suggesting that the

basic conditions required in the reaction are incompatible with the stability of $Cu_3(BTC)_2$.

Another catalytic system was developed based on $Cu_3(BTC)_2$ in the presence of TEMPO and NMI as co-catalyst for aerobic alcohol oxidation.[60] Under optimal conditions, BA was converted in 94 % yield in acetonitrile under oxygen atmosphere at 70 °C. This catalytic system was also able to convert other various primary alcohols to their respective aldehydes in high yields. Furthermore, three consecutive oxidation reactions, each of them requiring fresh aliquots of TEMPO and NMI, were performed using $Cu_3(BTC)_2$/TEMPO/NMI for the oxidation of BA. The yield of benzaldehyde decreased to 67 % after the second run, and the yield further dropped significantly to 15 % after the third run. In addition, the solution turned blue after second run, thus, suggesting copper leaching. Therefore, although the activity and scope of $Cu_3(BTC)_2$/TEMPO/NMI is interesting, stability under reaction conditions is still unsatisfactory.

$Cu_3(BTC)_2$ of different crystal sizes (Figure 12) were synthesised and their activity was examined in the aerobic oxidation of BA.[61] One of these samples, Cu-MOF-2, exhibited in the presence of TEMPO > 99% BA conversion and selectivity at 75 °C using Na_2CO_3 as base in acetonitrile. In contrast to the behaviour of BA, efforts to oxidize 1-phenylethanol and diphenylcarbinol using Cu-MOF-2 and TEMPO failed, even at 120 °C. This higher reactivity of primary versus secondary benzylic alcohols follows general trends for many solid catalysts and indicates that the active sites are spatially encumbered. In agreement with this rationalization, the increase of the size of aromatic rings of primary aromatic alcohols decreased the yields of the corresponding aldehydes. For example, the aerobic oxidation of BA (4.3 Å), 2-naphthalenemethanol (6.7 Å) and 9-anthracenemethanol (9.2 Å) in the presence of Cu-MOF-2 gave 99, 76 and 33 % yield under identical conditions. These data suggest that the reaction occurs within the pores of Cu-MOF-2. The catalyst was recycled fifteen times and no leaching of copper was detected in the solution. No attempts were made for the aerobic oxidation of aliphatic and cyclic alcohols under the present experimental conditions.

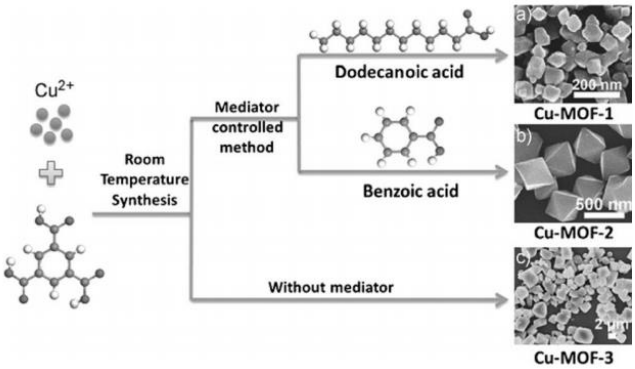

Figure 12. Synthetic procedures used to obtain $Cu_3(BTC)_2$ of different crystallite dimensions. The sizes of the Cu MOFs are 90 nm, 400 nm and several μm for Cu-MOF-1, Cu-MOF-2 and Cu-MOF-3, respectively. These three Cu-MOF samples had surface areas of 1409, 1391, and 1129 m^2g^{-1}, respectively. Reproduced from ref. [61] with permission from Wiley.

A mesoporous $Cu_3(BTC)_2$ catalyst was prepared via creating MOF nanocrystals containing PEG (Scheme 5) and its activity was studied for the aerobic oxidation of BA to benzaldehyde.[62] PEG served as the reaction medium to induce the room temperature crystallization of nanosized MOF, allowing controlling the crystallization rate of the framework, during which the triblock copolymer P104 ($EO_{27}PO_{61}EO_{27}$) micelles template the generation of mesopores (Scheme 5). Simultaneously, PEG molecules can be immobilized in the MOF pores through hydrogen bonding interactions with the BTC, acting as a strut to prevent the collapse of the mesopores. The mesoporous MOF nanocrystals stabilized by PEG were finally obtained after removing the surfactant and solvent (Scheme 5). Powder XRD pattern of the mesoporous MOF is in agreement with that of HKUST-1 [$Cu_3(BTC)_2$]. SEM images indicated that the crystals have a typical morphology of bipyramidal octahedron. The TEM images revealed that the MOF octahedron is constructed from ultrafine crystallites (2–3 nm), forming a disordered mesoporous structured particle with pore size of 3-4 nm. The catalytic activity of the as-synthesised mesoporous $Cu_3(BTC)_2$ based on the use of PEG as medium and P104 as template agent showed complete conversion of BA in the presence of TEMPO and oxygen in acetonitrile at 75 °C. It was claimed that the activity of this catalyst is superior than the activity of commercial $Cu_3(BTC)_2$ for the aerobic oxidation of BA,[59] but, however, it is always appropriate to compare the activities of catalysts in terms of TON/TOF. This enhanced activity of PEG-stabilized $Cu_3(BTC)_2$ is believed to be due to the smaller particle size and mesoporous structure of $Cu_3(BTC)_2$, which are favourable for the increased accessibility of catalytic active sites and diffusion of substrates and products. Hot filtration test indicated the absence of leached copper species having catalytic activity into the liquid phase during the reaction. The catalyst was reused for four cycles. No major difference was observed for between XRD patterns of the fresh $Cu_3(BTC)_2$ and four times reused sample, indicating that the structural integrity of the mesoporous Cu MOF was preserved. However, the activity of this catalyst was tested only with BA and no attempts were made to expand the substrate scope to other linear, cyclic, primary and secondary alcohols.

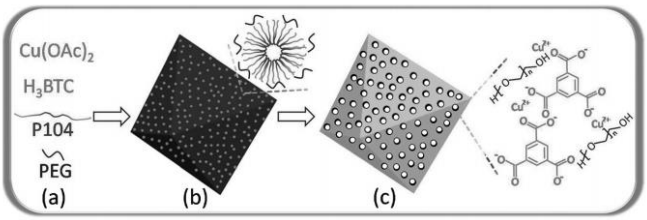

Scheme 5. Illustration showing the formation of PEG-stabilized mesoporous Cu MOF nanocrystals. Reproduced from ref. [62] with permission from Wiley.

Recently, a core–shell SPS–Cu(II)@$Cu_3(BTC)_2$ catalyst composed of a sulfonated-polystyrene (SPS) core, an active Cu(II) interface and a microporous $Cu_3(BTC)_2$ shell was developed and its activity for the aerobic oxidation of alcohols

by molecular oxygen under base-free conditions reported.[63] As shown in Figure 13, Cu(II) ions were first grafted onto a sulfonated polystyrene core to generate a well-defined active surface decorated with uniform active Cu(II) sites. Part of the -SO_3H grafted copper ions form the active surface and the rest of the –SO_3H provided acid groups to promote a high catalytic activity. Furthermore, some of the Cu(II) ions linked with the sulfonic group further coordinated with BTC ligands to generate a microporous MOF shell. The $Cu_3(BTC)_2$ nanocrystals deposited on the surface of the SPS microsphere exhibit a typical octahedron-like structure with a mean diameter of 80 nm. The HRTEM image further reveals that the SPS–Cu(II)@$Cu_3(BTC)_2$ particles present a core–shell structure with a relatively thin shell of about 300 nm composed of fine $Cu_3(BTC)_2$ nanoparticles. The HAADF-STEM image of a SPS–Cu(II)@$Cu_3(BTC)_2$ microsphere along with the corresponding elemental mapping of S and Cu in the SPS–Cu(II)@$Cu_3(BTC)_2$ material indicated that the surface of the polystyrene microsphere contains sulfonic acid groups, and the SPS core is uniformly wrapped by the Cu element. The BET surface area of the SPS–Cu(II)@$Cu_3(BTC)_2$ composite was 227.62 m^2g^{-1}. SPS–Cu(II)@$Cu_3(BTC)_2$ composite exhibited 99 % yield of benzaldehyde in the oxidation of BA using TEMPO as cocatalysts in acetonitrile at 75 °C with oxygen as oxidant. Under identical conditions, the use of SPS–Cu(II) also afforded 99 % yield of benzaldehyde, thus indicating that the Cu(II) interface can act as the main catalytically active component of the SPS–Cu(II)@$Cu_3(BTC)_2$ catalyst. The recyclability of the SPS–Cu(II) and SPS–Cu(II)@$Cu_3(BTC)_2$ catalysts was examined for the selective oxidation of BA. The SPS–Cu(II)@$Cu_3(BTC)_2$ catalyst remained active for ten recycles. The powder XRD patterns and FESEM images of the catalyst after ten cycles show that the overall structure of the material remains intact, indicating that the SPS–Cu(II)@$Cu_3(BTC)_2$ catalyst is stable under these conditions. In contrast, benzaldehyde yield decreased significantly to 68 % after three cycles with SPS–Cu(II) sample, thus showing the superior performance of the core-shell catalyst. SPS–Cu(II)@$Cu_3(BTC)_2$ performs as heterogeneous catalyst under these conditions. Although this core-shell catalytic system based on $Cu_3(BTC)_2$ showed high yields for the substituted BAs, poor yield was observed for 1-phenylethanol, cyclohexanol and cyclopentanol under identical conditions.

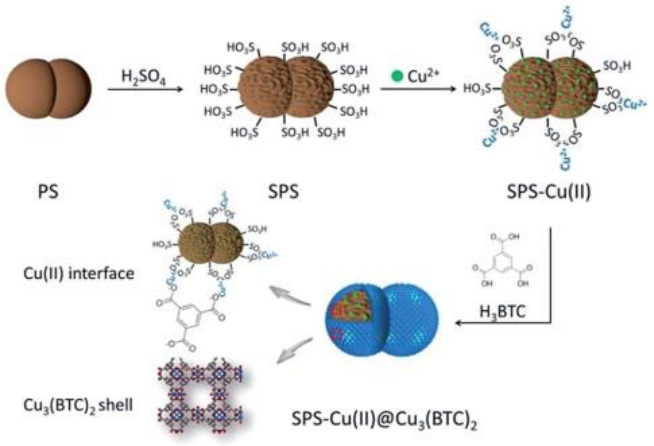

Figure 13. Synthesis process of the SPS–Cu(II)@$Cu_3(BTC)_2$ composite. Reproduced from ref. [63] with permission from Royal Society of Chemistry.

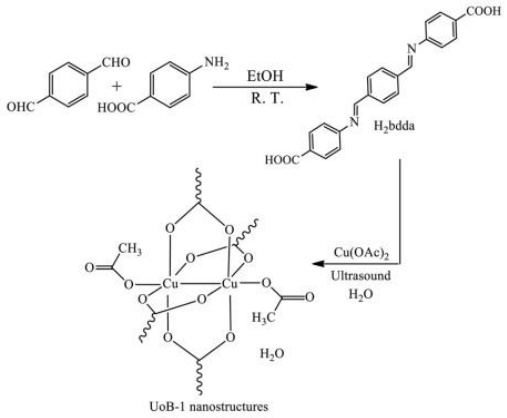

Figure 14. Synthesis of UoB-1 from Schiff base as organic linker and paddle wheel arrangement of Cu_2 metal nodes. Reproduced from ref. [64] with permission from Elsevier.

A new nanostructured copper-based MOF with a Schiff base ligand (Figure 14), Cu_2 (BDDA)$(OAc)_2 \cdot H_2O$ (UoB-1; UoB: University of Birjand) was prepared via ultrasound assisted method and its activity was evaluated in BA oxidation.[64] The TEM images of UoB-1 indicated that the most of the crystallites were spherical in shape with the average particle diameter of 51 nm. The use of UoB-1 as catalyst showed 95 % yield of benzaldehyde using TBHP as oxidant at 45 °C under solvent-free conditions. A series of BAs were converted to their respective aromatic carbonylic compounds in high yields. In this way, this catalyst afforded 80 % acetophenone under identical conditions, but requiring longer reaction time. The catalyst was used for six consecutive reactions without significant loss of its activity. The TEM image of UoB-1 nanostructures after being reused for six cycles displayed no significant changes in the particle size. ICP-AES analysis indicated no detectable Cu in the liquid phase.

Reactions of 5-{(pyridin-4-ylmethyl)amino} isophthalic acid (H_2L1) with copper(II), zinc(II), and cadmium(II) resulted in the formation of MOFs, namely $[\{Cu(L1)(DMF)\}\cdot DMF\cdot H_2O]_n$, $[Zn(L1)(H_2O)]_n$, and $[Cd(L1)]_n$. The MOFs

$[\{Cu(L1)(DMF)\}\cdot DMF\cdot H_2O]_n$ and $[Zn(L1)(H_2O)]_n$ have 2D structures, whereas $[Cd(L1)]_n$ features a 3D network with a bimetallic Cd_2 core acting as a secondary building unit (Figure 15).[65] The catalytic activity of these MOFs was tested in the oxidation of BA and 1-phenylethanol using TBHP as oxidant under solvent-free, microwave conditions at 100 °C. Among these MOFs, $[\{Cu(L1)(DMF)\}\cdot DMF\cdot H_2O]_n$ exhibited the highest activity for BA oxidation, reaching 81 % yield of benzaldehyde with TOF value of 811 h^{-1} which is much higher compared with copper nitrate trihydrate as homogeneous catalyst (172 h^{-1}). Under identical conditions, this catalyst showed 98 % yield of acetophenone with the TOF value being 983 h^{-1}. The benzaldehyde yield decreased from 81 to 3.8 or 1.3 %, respectively, in the presence of Ph_2NH or $CBrCl_3$. Similarly, the yield of acetophenone significantly reduced from 98 to 2.6 or 2.9 %, respectively, in the presence of Ph_2NH or $CBrCl_3$. These data suggest that the oxidation reaction promoted by this Cu MOF is a radical mediated pathway. Although this catalyst shows higher activity compared to $Cu_3(BTC)_2$ which is able to catalyze the TEMPO-assisted aerobic oxidation of BA to benzaldehyde with 99 % yield at 70 °C[61] and to 100 % yield of benzaldehyde in the presence of mesocellular MOFs,[83] the activity of $[\{Cu(L1)(DMF)\}\cdot DMF\cdot H_2O]_n$ could be further improved in terms of utilizing greener oxidant, like molecular oxygen, and expanding the scope to linear, cyclic, primary and secondary alcohols. The catalyst was recycled for three runs without much decay in its activity and leaching experiments did not show any copper in the solution. Furthermore, powder XRD patterns of the fresh and three times reused catalyst did not show any noticeable change in their crystallinity.

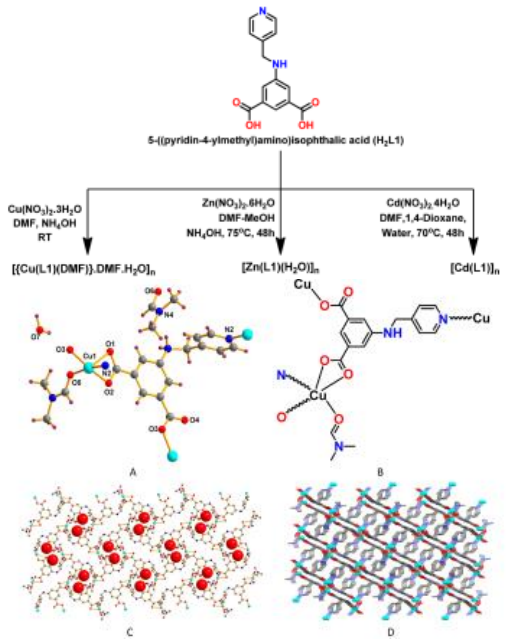

Figure 15. Building units of Cu(L1)DMF framework (A and B) showing ligand and reagents used in the synthesis of these MOFs containing either Cu, Zn or Cd. The bottom frames show two-dimensional structure of framework (water molecules are indicated as red balls) (C) and three-dimensional packing (D) of Cu(L1)DMF. Reproduced from ref. [65] with permission from American Chemical Society.

Cu-MOF-74 was used as solid catalyst for the aerobic BA oxidation under oxygen atmosphere at 70 °C in the presence of TEMPO and DMAP as co-catalysts, observing 89 % yield of benzaldehyde under optimal conditions.[66] A series of substituted BAs were converted in high yields under identical conditions. The catalytic activity of Cu-MOF-74 was maintained in two consecutive runs, but however, there was no evidence to support the catalyst stability under this experimental condition by characterizing the spent catalyst. Also, no efforts were made to oxidize secondary alcohols under this experimental condition.

Recently, mixed linker Cu(II)-based MOF, $\{[Cu_2(1,2\text{-}BDC)_2(FBTX)_2]\cdot 3H_2O\}_n$ (Cu-FMOF) was hydrothermally synthesized and its activity evaluated in the oxidation of 4-methoxybenzyl alcohol.[67] A complete conversion of 4-methoxybenzyl alcohol with >99 % of the corresponding aldehyde was achieved in the presence of 10 mol% Cu-FMOF and TEMPO as cocatalysts using Na_2CO_3 in acetonitrile at 75 °C under air atmosphere. However, the same oxidation reaction has been reported with 24 mol% $Cu_3(BTC)_2$ catalyst, where relatively lower activity was observed.[59] In another work, Wang et al., have reported the catalytic oxidation of 4-methoxybenzyl alcohol with 17 mol% small particle size $Cu_3(BTC)_2$ (Cu-MOF-2, see Figure 12), reaching 99 % conversion at 75 °C.[61] It is appropriate to mention here that the catalytic performance of different solids must be compared based on their TON/TOF values, rather than on substrate conversion, since each experiment is performed under different conditions, including Cu-to-substrate mole ratio. Furthermore, the activity of Cu-FMOF was tested for a series of substituted BA, observing moderate to high yields. However, the activity of Cu-FMOF was not tested for linear, cyclic, primary or secondary aromatic alcohols, thus appearing as a catalyst with narrow scope. On the other hand, the catalyst maintained its activity with almost no decrease in five consecutive cycles, but continued addition of TEMPO and base in each run was necessary. Hot filtration experiments support the absence of leaching of active sites. Comparison of the FT-IR spectrum and powder XRD patterns between the fresh and the recycled catalyst provides evidence of the maintenance of the crystallinity. XPS analysis confirmed that no change in the oxidization state for copper occurs during the course of reaction.

Besides Cu, Co is other transition metal with general catalytic activity to promote oxidation. In this way, a series of MOFs with cobalt, copper and iron as central metal ions and BTC as a ligand were synthesized (denoted M-BTC) and their activity was tested in the selective oxidation of BA.[68] The extended framework of M-BTC (M = Co, Cu, Fe) is established through linked metal centres and BTC ligands.[84] The BTC ligand acts as a trigonal planar ligand connecting the diatomic metal clusters with an open framework (Figure 16). The BET surface area of $Cu_3(BTC)_2$, Fe(BTC) and $Co_3(BTC)_2$ was 917, 369 and 18 m^2g^{-1} respectively. Under the optimal reaction conditions, the conversion of BA in the presence of $Co_3(BTC)_2$ reached to 92.9

% with the selectivity of benzaldehyde of 97 % at 95 °C in DMF with air as oxidant. In contrast, compared to $Co_3(BTC)_2$, the other two catalysts in the series, namely, $Cu_3(BTC)_2$ and Fe(BTC) showed 24 and 11 % conversions, respectively, under similar conditions. These data clearly suggest that the activity of a catalyst does not depend on the BET surface area, although certainly the low specific surface area of $Co_3(BTC)_2$ should have deserved a more detailed study, particularly in connection with its remarkable catalytic activity and the possibility that the reaction occurs on the external surface of the crystallites. However, it is well documented that Co-based[85] and Fe-based[86] compounds can be highly efficient oxidation catalysts. $Co_3(BTC)_2$ was reused for three cycles decreasing the activity of this catalyst in the second and third cycles to 90 and 88 % BA conversion, respectively. To understand this activity decay, powder XRD showed a major change in its crystallinity after two consecutive uses of $Co_3(BTC)_2$ compared to fresh catalyst. These data indicate the poor catalyst stability under the reaction conditions even in the absence of base.

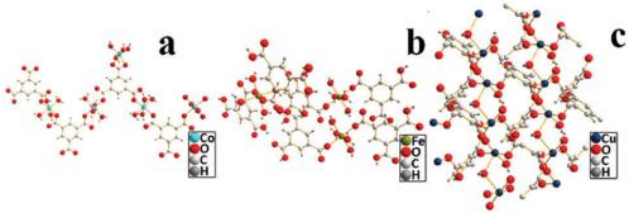

Figure 16. Illustration of the structure of (a) $Co_3(BTC)_2$, (b) Fe(BTC) and (c) $Cu_3(BTC)_2$ MOFs. Reproduced from ref. [68] with permission from Royal Society of Chemistry.

Recently, a series of mixed linker MOFs containing different first-row transition metals, namely, $M(BDC)(TED)_{0.5}$ (M = Co, Zn, Ni, Cu), has been reported and their activity was studied in the oxidation of BA.[69] The BET surface area of $Co(BDC)(TED)_{0.5}$, $Cu(BDC)(TED)_{0.5}$, $Zn(BDC)(TED)_{0.5}$ and $Ni(BDC)(TED)_{0.5}$ was 1510, 1197, 1592 and 1763 m^2/g, respectively. Among these catalysts, $Co(BDC)TED)_{0.5}$ exhibited 81 % conversion of BA with 99 % selectivity of benzaldehyde in DMF at 90 °C using oxygen as oxidant. It is interesting to note that this experimental condition does not require either TEMPO or a base to promote the reaction. In contrast, the use of $Cu(BDC)(TED)_{0.5}$, $Zn(BDC)(TED)_{0.5}$ and $Ni(BDC)(TED)_{0.5}$ as catalysts for the oxidation of BA to benzaldehyde gave 8.8, 5.6 and 25.2 % conversions, respectively, under identical conditions which were much lower than the conversion achieved with $Co(BDC)(TED)_{0.5}$. The different catalytic activity observed over isostructural $Cu(BDC)(TED)_{0.5}$, $Co(BDC)(TED)_{0.5}$, $Ni(BDC)(TED)_{0.5}$ and $Zn(BDC)(TED)_{0.5}$ indicated that the catalytic activity is mainly dependent on the metal ions in the MOFs. Compared with Cu^{2+}, Zn^{2+} and Ni^{2+}, Co^{2+} sites of $Co(BDC)(TED)_{0.5}$ are the most efficient catalytic active sites to activate molecular oxygen in the absence of radical co-catalysts. This kind of activity has been observed earlier for molecular metal complexes. For instance, $Co(acac)_2$ (acac: acetylacetonate) shows better catalytic activity than $Cu(acac)_2$, $Ni(acac)_2$, $Fe(acac)_2$ and $Mn(acac)_2$ for the selective oxidation of BA.[87] $Co(BDC)(TED)_{0.5}$ was recycled three cycles without any decay in conversion and selectivity. Hot filtration test is in accordance with the heterogeneity of the reaction. There were no differences in the crystallinity between fresh and three time recycled catalyst. However, the activity of this catalyst was studied only for BA and efforts should be made to examine the activity for oxidation of much more challenging alcohols.

A porous Co(II)-MOF was synthesized under solvothermal conditions by the reaction of a bent imidazole-bridged ligand (L, see structure in Scheme 6) and BDC with $Co(OAc)_2$ to obtain Co(L)(BDC)(MeOH).[70] Subsequently, desolvated $Co(L)(BDC)_2$ MOF (see structure in Scheme 6) was reported as heterogeneous catalyst for BA oxidation at 60 °C with TBHP as oxidant, reaching 88 % conversion with 91 % selectivity to benzaldehyde. Furthermore, 4-methoxybenzyl alcohol was oxidized in 98 % conversion with 31 % selectivity to 4-methoxybenzaldehyde and 69 % selectivity to the corresponding benzoic acid. Similarly, 4-nitrobenzyl alcohol was oxidized in 91% conversion with 76% selectivity to the corresponding aldehyde and 24 % of the acid. On the other hand, 1-phenylethanol was oxidized to acetophenone in 95 % conversion under identical conditions. This catalyst was recycled for three cycles and powder XRD did not show any significant difference between fresh and reused catalysts.

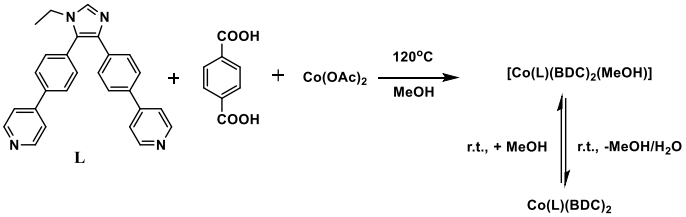

Scheme 6. Synthesis of $Co(L)(BDC)_2$ MOF and structure of bent imidazole ligand (L).

Phosphonate ligands have been extensively used to construct MOFs.[88] The versatility of the phosphonate building blocks allows the use of a series of P-containing linkers to create a library of new materials with interesting properties and diverse applications.[89] Metal carboxylate-based MOFs often suffer from instability under reaction conditions.[90] In this regard, phosphonate linkers have demonstrated advantages in terms of framework stability of the materials they form. This is due to the higher charge of the coordinating group, the higher number of atoms involved in bonding and the tendency to form more than one oxygen-metal bond per oxygen atom.[91] Among the various phosphonate ligands, N,N'-pipirazine bis(methylenephosphonic) acid has been used widely for the design of MOFs such as STA-12.[92] In this context, a series of phosphonate based MOFs like STA-12(Co), STA-12(Ni) and STA-12(Ni +20% Co) have been synthesised and their activity tested for alcohol oxidation.[71] The catalytic activity of these materials was examined in terms of solvent, oxidant, reaction temperature, and time for the oxidation of 4-chlorobenzyl alcohol. Thus, STA-12(Co) gave 50 % yield of 4-chlorobenzaldehyde using TBHP as oxidant in ethyl acetate as solvent at 60 °C. Hot filtration experiment indicated the heterogeneity of the reaction. STA-12(Co) was recycled for five runs for the oxidation of 1-phenylethanol to acetophenone without any noticeable decay in activity. Powder XRD confirmed

the structural integrity of the reused catalyst compared to the fresh catalyst.

A series of Ce(IV)-based MOFs isostructural to UiO-66 were synthesised under mild conditions and short reaction times using different linker molecules of various sizes and functionalities and their activity was tested in the aerobic BA oxidation.[72] Among the series of catalysts tested under different experimental conditions, Ce-UiO-66-BDC (activated at 220 °C) adding TEMPO as co-catalyst exhibited 88 % conversion at 110 °C in acetonitrile while a control experiment only with TEMPO resulted in 7 % benzaldehyde. In contrast, Ce-UiO-66-BDC/TEMPO activated at 180 °C afforded only 29 % conversion of BA under identical conditions. These data illustrate how significantly the performance of these catalysts, and any MOF in general, can be influenced by the activation process prior to the catalytic test. This enhanced activity due to the higher activation temperature is attributed to the removal of strongly adsorbed guest molecules and possible cluster dehydration as evidenced from the TGA data. This desorption should lead to the creation of open coordination sites analogous to the situation in Zr-UiO-66. Powder XRD pattern did not show any noticeable change between fresh and the recovered Ce-UiO-66-BDC. Hot filtration experiment is in agreement with the heterogeneity of the process. The synergistic effect between Ce-UiO-66-BDC and TEMPO was not observed for Zr-UiO-66 and TEMPO (~10 % yield), reflecting the well-known fact of how the nature of the transition metal can determines the catalytic activity. Further data is required to assess the scope of the catalyst to other types of substrates.

4. Photocatalytic oxidation

MOFs are currently being intensively investigated as photocatalysts.[93, 94] Light excitation promotes as a general phenomenon, electron transfer from the ligand to the metal cluster and this charge migration can serve to promote chemical reactions. Among the most general photocatalytic reactions, one that is well established is photooxidation and, more specifically, oxidation of BAs to benzaldehydes. Thus, MOFs have been widely used as photocatalysts to promote the oxidation of BA to benzaldehyde under aerobic conditions.[94] In fact, this is a model reaction that can be used to rank the photocatalytic activity of different materials, by monitoring the yield of benzaldehyde formed under certain irradiation conditions.

A series of mixed-linker zirconium-based UiO-66 MOFs containing 2-amino-1,4-benzenedicarboxylate as the primary linker and 2-X-1,4-benzenedicarboxylate (X = H, F, Cl and Br) as a secondary linker was prepared and their photoactivity was studied in the oxidation of BA under visible-light irradiation.[73] Powder XRD patterns showed that the mixed-linker UiO-66 MOFs are crystalline and isoreticular to the parent UiO-66. The conversion of BA was 18.4 % with NH_2-UiO-66 as catalyst. Among the various catalysts examined, NH_2-UiO-66-F, NH_2-UiO-66-Cl, and NH_2-UiO-66-Br exhibited 53.9, 38.2, and 43.4 % conversions of BA under identical conditions. These experiments clearly establish that partial replacement of BDC linkers by halogenated analogues (X-BDC, X = F, Cl, Br) leads to a four- to five-fold enhancement of the photocatalytic activity for the BA oxidation in comparison to NH_2-UiO-66. It is proposed that this enhanced photocatalytic activity is due to the stabilization of the superoxide radical anion on the Zr^{3+} connected to the halogenated linkers, decreasing the recombination rate of the photogenerated electrons and holes. Other possible reasons for this enhancement in the photocatalytic activity could be related to the preferential interaction of the halogen groups with BA molecules driving the equilibrium of the reaction to benzaldehyde.

Recently, the photocatalytic titanium-oxo cluster and photosensitizing porphyrinic linker (TCPP: tetrakis(4-carboxyphenyl)porphyrin) were assembled to obtain PCN-22.[74] The conversion of BA to benzaldehyde reached to 28 % in the presence of PCN and TEMPO under visible-light irradiation with 100 % selectivity with a TON of 100. The photocatalyst was reused for three consecutive runs without any decay in its activity. The photocatalytic performance of PCN-22 was compared with TiO_2, TCPP, mechanical mixture of TiO_2 and TCPP and PCN-224 (composed of Zr_6O_8 clusters and TCPP ligands) under identical conditions (Figure 17). As it can be seen in Figure 17, PCN-22 exhibits much higher activity than the rest of the controls. The lower activity of PCN-224 may be attributed to the large energy gap and fast charge recombination of the Zr_6O_8 cluster. On the other hand, the lower activity observed by the physical mixture of TiO_2 and TCPP can be ascribed to the aggregation of the active sites. In contrast, the highly porous structure with crystalline ordering of chromophores and acceptors of PCN-22 makes each catalytic centre accessible to the substrates.

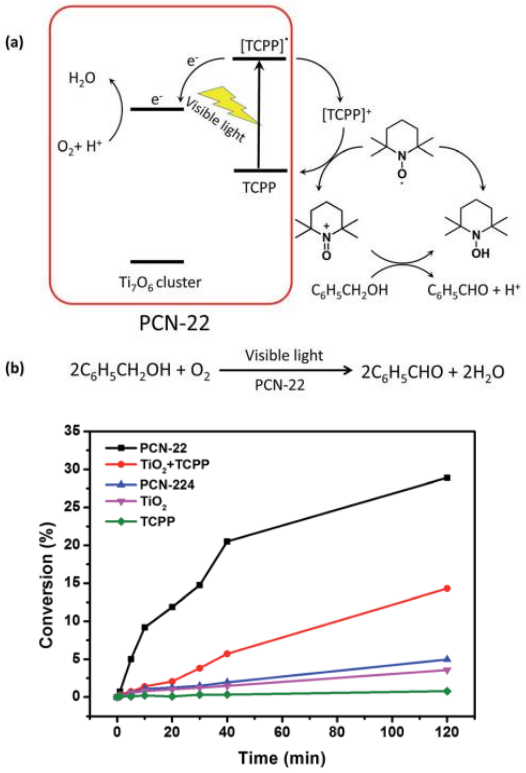

Figure 17. (a) Proposed mechanism for PCN-22/TEMPO system and (b) reaction catalyzed by PCN-22 (top); Time course of BA

oxidation catalyzed by different photocatalysts (bottom). Reproduced from ref. [74] with permission from Royal Society of Chemistry.

Mesoporous HKUST-1 decorated with amorphous TiO_2 nanoparticles was reported as a photocatalyst for the selective aerobic oxidation of alcohols under sunlight irradiation.[75] Different amounts of P123 were used to determine the optimum surfactant concentration in the surfactant-assisted synthesis of HKUST-1 (SHK represents surfactant assisted synthesis of HKUST-1). On the other hand, a control HKUST-1 sample was also prepared in the absence of structure-directing agent P123. TEM images suggested that SHK consists of ordered mesoporous domains of small parent MOF crystallites having microporous structure. Powder XRD, IR, and SEM analysis supported that the crystallinity and structure of the parent MOF remain intact after titania decoration. The photocatalytic activity of these TiO_2-MOF nanocomposite materials was studied in the aerobic oxidation of 4-methylbenzyl alcohol in CH_3CN under sunlight irradiation. The 70Ti@SHK2 photocatalyst having 70 % TiO_2 was able to achieve up to 89 % conversion of 4-methylbenzaldehyde with high selectivity (> 93 %). The high photocatalytic reactivity of TiO_2-SHK materials arises to a large extent from their uniform mesostructure, implying that the reaction takes place inside the mesopores. Furthermore, TiO_2-modified SHK was also an active photocatalyst to transform primary and secondary benzylic alcohols into their corresponding carbonyl compounds with high selectivities (93-99 %) and moderate to high conversions (32–100 %). The recycled TiO_2@SHK2 photocatalyst still retains a large percentage of the initial activity of the fresh material upon sunlight irradiation. The partial decrease in photocatalytic activity was attributed to structural changes upon catalyst use. However, it is well known in the area that amorphous TiO_2 is generally much less photocatalytically active than crystalline anatase or even rutile phases and one improvement in the material would be to prepare an analogous sample having crystalline TiO_2 NPs.

5. MNPs@MOFs as active sites

Besides transition metal ions, supported MNPs of small size in the range of a few nanometers are also known to be highly active and general oxidation catalysts. Among the reactions that these MNPs can catalyze, the aerobic oxidation of alcohols, including BAs, is one that has attracted considerable attention. One of the main problems, besides the cost of some expensive metals, is stabilization of the small particle size under reaction conditions. Stabilization of small particle size is one of the main roles of the support and one of the possibilities that have been successful to avoid particle growth is incorporation of the MNPs inside the restricted cavities of a porous solid host.

MNPs supported on MOFs are one of the most efficient heterogeneous oxidation catalysts to achieve high product yields. Recently, the catalytic activity of various MOF catalysts[13] or Au NPs supported on MOFs[16] as heterogeneous solid catalysts for oxidation reactions, including oxidation of BA, has been reviewed. However, due to the fast progress of the field, some more recent articles dealing with MNPs encapsulated within MOFs as catalysts for BA oxidation have appeared after publication of these reviews. The following papers have been selected to illustrate how MNPs provide high activity for this reaction.

Pt@MOF-177 has been examined as a catalyst for the aerobic oxidation of BA under base-free conditions resulting in 50 % conversion with a TON of 968.[76] The particle size of Pt was in the range of 2-5 nm. However, the recyclability of Pt@MOF-177 was unsatisfactory. After the first cycle, the Pt@MOF-177 nanocomposite was subjected to powder XRD, observing the absence of reflections in the 2θ range value of 5-20^o corresponding to MOF-177 structure. This indicates the breakdown of the MOF host lattice during the oxidation reaction. A second cycle with the same catalyst gave almost no activity in the oxidation process.

Contrast to the poor performance of Pt@MOF-177, in one of the seminal reports, Au NPs incorporated on MIL-101(Cr) by colloidal deposition with polyvinylpyrrolidine (PVP) as protecting agent exhibited the highest catalytic activity for aerobic oxidation of alcohols to aldehydes under base-free conditions.[77] This high activity can be attributed to the low mean diameter of Au NPs (2.3 nm) that can be achieved following the appropriate MIL-101(Cr) (see structure in introduction section) incorporation procedure. The use of Au/MIL-101(Cr) exhibited in almost complete conversion (>95 %) and selectivity (>99 %) in the aerobic oxidation of BAs to their corresponding aldehydes. On the other hand, secondary aliphatic alcohols showed higher activity than primary counterparts, a trend that is often not observed in porous catalysts due to steric effects. Furthermore, alcohols having heteroatoms were also oxidized with high conversion and selectivity. No leaching of Au was observed under the experimental conditions and Au particle size before and after the use of the material as catalyst for oxidation reaction remains unaltered as evidenced by TEM analysis. The Au/MIL-101(Cr) material gave identical yield (>99 %) up to the sixth cycle for the oxidation of 4-methoxybenzyl alcohol. This catalyst showed a very high TOF value of 29 300 h^{-1} for the aerobic oxidation of 1-phenylethanol.

The high catalytic activity of this Au-containing MOF arises from the combination of a series of possible factors, including i) the robust structure of MIL-101(Cr) that can withstand water and organic solvents, ii) the large pore size of MIL-101 (1.1 and 1.5 nm windows) facilitating mass transfer of reactant/product molecules inside the pores and iii) the small Au NP size and its stability when encapsulated inside MIL-101(Cr). It is always desirable that all the MOFs used as heterogeneous catalysts fulfil these conditions. In another precedent, Au/PMA-MIL-101 with Au content of 1.5 wt % and a particle size of 2.5 nm was reported as heterogeneous catalyst for the oxidation of BA under air atmosphere using K_2CO_3 as base reaching 60 % conversion with a TOF of 7 min^{-1}.[78] These findings illustrate that the particle size, nature of MOF and the reaction conditions are extremely important to achieve high activity in the aerobic oxidation of BA.

A sample of highly dispersed Pd NPs deposited on MIL-101 prepared following an impregnation method using colloidal

MNPs was obtained and its activity was tested in the liquid-phase aerobic oxidation of a wide range of alcohols under base-free and mild conditions.[79] TEM images revealed that the particle size of Pd was 2.5±0.5 nm in 0.35 % Pd loading in Pd/MIL-101 sample. Among the various catalysts with various Pd loadings on MIL-101 tested, 0.35 % Pd/MIL-101 afforded 99 % conversion and selectivity in the oxidation of cinnamyl alcohol in toluene at 80 °C under aerobic condition. Under the optimized reaction condition, the solvent-free aerobic oxidation of BA gave a remarkably high TOF value of 16900 h^{-1} at 160 °C. It is interesting to note that the TOF value achieved by Pd/MIL-101(Cr) is higher than those reported for samples of Pd supported on active carbon that afforded lower TOF values in the range of 15235 h^{-1} for the conversion of BA at 160 °C.[95] However, the catalytic activity of 0.35 % Pd/En-MIL-101(Cr) (Pd NPs supported on ethylenediamine grafted on MIL-101) was significantly suppressed to 45 % conversion with 99 % selectivity under identical conditions. This indicates that the open Cr sites might play an important role in promoting the oxidation of alcohols in Pd/MIL-101(Cr). Reusability experiments showed no efficiency loss in the catalytic activity for the aerobic oxidation of cinnamyl alcohol up to five runs. Furthermore, atomic absorption spectroscopy chemical analysis did not allow the detection of Pd in the reaction solution. Powder XRD of the fresh and five times used samples showed no appreciable changes in the crystallinity of the MIL-101(Cr) material.

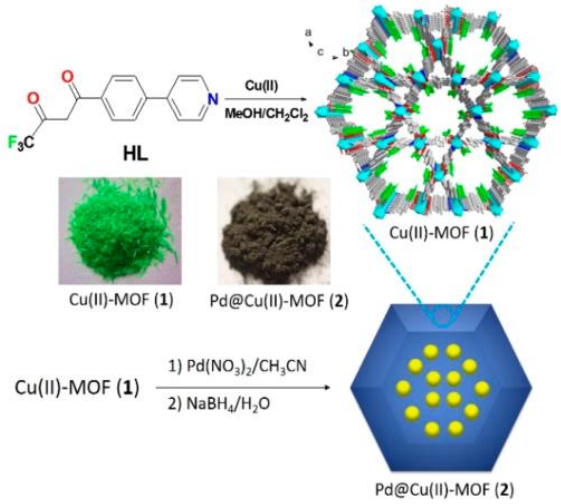

Figure 18. Synthesis of Cu(II)-MOF and Pd@Cu(II)-MOF. Reproduced from ref. [80] with permission from American Chemical Society.

A new 3D porous Cu(II)-MOF with a NbO motif was prepared using a ditopic pyridyl substituted diketonate ligand and $Cu(OAc)_2$. Subsequently, Pd NPs were loaded on Cu(II)-MOF to obtain a hybrid material of Pd@Cu(II)-MOF (Figure 18) through solution impregnation method.[80] HRTEM analysis indicated that the Pd NPs were crystalline and highly dispersed with an average particle size of ca. 2 nm. The catalytic activity of Pd@Cu(II)-MOF was tested in the oxidation of BA under air atmosphere at 130 °C in xylene, reaching 95 % conversion with 99 % selectivity of benzaldehyde. The TON and TOF values achieved with this catalyst were 19 and 0.76 h^{-1}, respectively. No leaching of Pd was detected and, thus, it is can be assumed that the material is acting as heterogeneous catalyst. The Pd@Cu(II)-MOF was recycled seven times for BA oxidation. The size and dispersion of the Pd NPs in Pd@Cu(II)-MOF did not show any aggregation after six runs. The conversion, however, decreased to 85 % in the seventh run, indicating the partial deactivation of Pd@Cu(II)-MOF. This catalytic data can be understood based on the information provided by HRTEM analysis showing that some of the Pd NPs in Pd@Cu(II)-MOF began to aggregate, which could be the reason for the lower activity of Pd@Cu(II)-MOF after six runs. In addition, inductively coupled plasma elemental analysis indicated that the amount of Pd NPs in Pd@Cu(II)-MOF does not show significant change after six runs, while the amount of Pd dropped from 5.1 wt% in the fresh catalyst to 3.85 % after the seventh cycle, which could be an additional reason for catalyst deactivation. On the other hand, powder XRD patterns of fresh and six time reused Pd@Cu(II)-MOF indicated that the structural integrity is well maintained under the reaction conditions.

Overall, the available activity data show that noble MNPs, particularly Au and Pd, of particle size below 3 nm incorporated inside robust MOF structures are highly active to promote the aerobic oxidation of BA and other alcohols. A further improvement in the area would be analogous systems based on abundant first-row transition metals exhibiting similar high catalytic activity for aerobic oxidations than noble MNPs.

6. Conclusions

The present review has shown the state of the art with regard to BA oxidation promoted by MOFs. As it can be seen there, the most active materials at present are those in which metal NPs, particularly, Au are embedded inside structurally robust, highly porous MOFs, namely MIL-101(Cr). There is still a room for developing non-noble metal catalysts based on MOFs and particularly for using the metallic nodes or organic linkers as active sites. In the last case, the strategy that has been used so far and the one that has given better results is to buid transition metal complexes using the linker as anchoring point. Also, the current state of the art with respect to light assisted aerobic oxidations still allows an opportunity for developing more efficient systems under visible light irradiations. At the present, the yields of photoassisted reactions are generally below 50 % due to the low conversions that have been achieved.

The target in the area should be to apply MOFs for reactions that have industrial interest, particularly in the production of fine chemicals where soluble transition metals are currently used as homogeneous catalysts. Benzaldehyde, vanillin and related flavours as well as aliphatic aldehydes due to their uses as fragrances and synthetic intermediates are obvious targets. The purpose is to show that MOFs can exhibit activity and stability high enough to be applicable in industrial processes.

Conflicts of interest

There are no conflicts to declare

Acknowledgements

AD thanks the University Grants Commission (UGC), New Delhi, for the award of an Assistant Professorship under its Faculty Recharge Programme. AD also thanks the Department of Science and Technology, India, for the financial support through Extra Mural Research Funding (EMR/2016/006500). Financial support by the Spanish Ministry of Economy and Competitiveness (Severo Ochoa and CTQ2015-69153-CO2-1) is gratefully acknowledged.

Notes and references

1. D. Farrusseng, S. Aguado and C. Pinel, *Angew. Chem., Int. Ed.*, 2009, **48**, 7502−7513.
2. J. Liu, L. Chen, H. Cui, J. Zhang, L. Zhang and C.-Y. Su, *Chem. Soc. Rev.*, 2014, **43**, 6011−6061.
3. J. Gascon, A. Corma, F. Kapteijn and F. X. Llabres i Xamena, *ACS Catal.*, 2014, **4**, 361−378.
4. A. H. Chughtai, N. Ahmad, H. A. Younus, A. Laypkov and F. Verpoort, *Chem. Soc. Rev.*, 2015, **44**, 6804−6849.
5. A. Dhakshinamoorthy, A. M. Asiri and H. Garcia, *Chem. Soc. Rev.*, 2015, **44**, 1922−1947.
6. A. Corma, H. Garcia and F. X. Llabres i Xamena, *Chem. Rev.*, 2010, **110**, 4606−4655.
7. Z. Fang, B. Bueken, D. E. De Vos and R. A. Fischer, *Angew. Chem., Int. Ed.*, 2015, **54**, 7234−7254.
8. J. Canivet, M. Vandichel and D. Farrusseng, *Dalton Trans.*, 2016, 4090−4099.
9. N. Stock and S. Biswas, *Chem. Rev.*, 2012, **112** 933-969.
10. W. Lu, Z. Wei, Z.-Y. Gu, T.-F. Liu, J. Park, J. Park, J. Tian, M. Zhang, Q. Zhang, T. Gentle III, M. Bosch and H.-C. Zhou, *Chem. Soc. Rev.*, 2014, **43**, 5561−5593.
11. M. L. Foo, R. Matsuda and S. Kitagawa, *Chem. Mater.*, 2014, **26**, 310−322.
12. M. Eddaoudi, J. Kim, N. Rosi, D. Vodak, J. Wachter, M. O'Keeffe and O. M. Yaghi, *Science*, 2002, **295**, 469-472.
13. A. Dhakshinamoorthy, A. M. Asiri and H. Garcia, *Chem. Eur. J.*, 2016, **22**, 8012-8024.
14. E. Roduner, W. Kaim, B. Sarkar, V. B. Urlacher, J. Pleiss, R. Glaser, W.-D. Einicke, G. A. Sprenger, U. Beifuß, E. Klemm, C. Liebner, H. Hieronymus, S.-F. Hsu, B. Plietker and S. Laschat, *ChemCatChem*, 2013, **5**, 82-112.
15. S. T. Madrahimov, J. R. Gallagher, G. Zhang, Z. Meinhart, S. J. Garibay, M. Delferro, J. T. Miller, O. K. Farha, J. T. Hupp and S. T. Nguyen, *ACS Catal.*, 2015, **5**, 6713-6718.
16. A. Dhakshinamoorthy, A. M. Asiri and H. Garcia, *ACS Catal.*, 2017, **7**, 2896−2919.
17. A. Dhakshinamoorthy, M. Alvaro and H. Garcia, *Catal. Sci. Technol.*, 2011, **1**, 856-867.
18. A. Dhakshinamoorthy, M. Opanasenko, J. Cejka and H. Garcia, *Adv. Synth. Catal.*, 2013, **355**, 247-268.
19. M. Opanasenko, M. Shamzhy, M. Lamac and J. Cejka, *Catal. Today*, 2013, **204** 94-100.
20. A. Dhakshinamoorthy, A. M. Asiri, J. R. Herance and H. Garcia, *Catal. Today*, 2017, DOI: 10.1016/j.cattod.2017.1001.1018.
21. S. D. Burke, *Danheiser, R. L., Eds. Handbook of Reagents for Organic Synthesis: Oxidizing and Reducing Agents; John Wiley & Sons: New York, 1999*.
22. G. Tojo and M. Fernandez, *In Oxidation of Alcohols to Aldehydes and Ketones; Tojo, G., Ed.; Springer: New York, 2010*.
23. R. A. Sheldon, I. W. C. E. Arends, G.-J. ten Brink and A. Dijksman, *Acc. Chem. Res.*, 2002, **35**, 774−781.
24. T. Mallat and A. Baiker, *Chem. Rev.*, 2004, **104**, 3037−3058.
25. R. E. Morris and J. Cejka, *Nature Chem.*, 2015, **7**, 381-388.
26. M. Polozij, E. Perez-Mayoral, J. Cejka, J. Hermann and P. Nachtigall, *Catal. Today* 2013, **204**, 101 - 107.
27. M. Polozij, M. Rubes, J. Cejka and P. Nachtigall, *ChemCatChem*, 2014, **6**, 2821-2824.
28. A. J. Howarth, Y. Liu, P. Li, Z. Li, T. C. Wang, J. T. Hupp and O. K. Farha, *Nature Rev. Mater.*, 2016, **1**, 15018-15032.
29. A. Dhakshinamoorthy, P. Concepcion and H. Garcia, *Chem. Commun.*, 2016, **52**, 2725--2728.
30. A. Dhakshinamoorthy, A. M. Asiri, P. Concepcion and H. Garcia, *Chem. Commun.*, 2017, DOI: 10.1039/c1037cc05221a.
31. A. Dhakshinamoorthy, M. Alvaro and H. Garcia, *Chem. Commun.*, 2010, **46**, 6476-6478.
32. A. Dhakshinamoorthy, M. Alvaro and H. Garcia, *Catal. Lett.*, 2015, **145**, 1600-1605.
33. A. Dhakshinamoorthy, M. Alvaro and H. Garcia, *Catal. Commun.*, 2017, **97**, 74-78.
34. F. Carson, V. Pascanu, A. B. Gûmez, Y. Zhang, A. E. Platero-Prats, X. Zou and B. Martin-Matute, *Chem. Eur.J.*, 2015, **21**, 10896 -10902.
35. M. F. Semmelhack, C. R. Schmid, D. A. Cortes and C. S. Chou, *J. Am. Chem. Soc.*, 1984, **106**, 3374−3376.
36. P. Gamez, I. W. C. E. Arends, J. Reedijk and R. A. Sheldon, *Chem. Commun.*, 2003, 2414−2415.
37. P. Gamez, I. W. C. E. Arends, R. A. Sheldon and J. Reedijk, *Adv. Synth. Catal.*, 2004, **346**, 805−811.
38. E. T. T. Kumpulainen and A. M. P. Koskinen, *Chem. Eur. J.*, 2009, **15**, 10901−10911.
39. J. M. Hoover and S. S. Stahl, *J. Am. Chem. Soc.*, 2011, **133**, 16901−16910.
40. J. M. Hoover, J. E. Steves and S. S. Stahl, *Nat. Protoc.*, 2012, **7**, 1161−1166.
41. G. Ragagnin, B. Betzemeier, S. Quici and P. Knochel, *Tetrahedron*, 2002, **58**, 3985−3991.
42. E. I. Solomon, U. M. Sundaram and T. E. Machonkin, *Chem. Rev.*, 1996, **96** 2563-2606.
43. G. Ferey, C. Mellot-Draznieks, C. Serre, F. Millange, J. Dutour, S. SurblJ and I. Margiolaki, *Science*, 2005, **309**, 2040-2042.
44. W. Xuan, C. Zhu, Y. Liu and Y. Cui, *Chem. Soc. Rev.*, 2012, **41**, 1677-1695.
45. S. S.-Y. Chui, S. M.-F. Lo, J. P. H. Charmant, A. G. Orpen and I. D. Williams, *Science*, 1999, **283**, 1148-1150.
46. J. H. Cavka, S. Jakobsen, U. Olsbye, N. Guillou, C. Lamberti, S. Bordiga and K. P. Lillerud, *J. Am. Chem. Soc.*, 2008, **130**, 13850-13851.
47. M. Kandiah, S. Usseglio, S. Svelle, U. Olsbye, K. P. Lillerud and M. Tilset, *J. Mater. Chem.*, 2010, **20**, 9848-9851.
48. S. Chavan, J. G. Vitillo, D. Gianolio, O. Zavorotynska, B. Civalleri, S. Jakobsen, M. H. Nilsen, L. Valenzano, C. Lamberti, K. P. Lillerud and S. Bordiga, *Phys. Chem. Chem. Phys.*, 2012, **14**, 1614-1626.
49. F. Carson, S. Agrawal, M. Gustafsson, A. Bartoszewicz, F. Moraga, X. Zou and B. Martin-Matute, *Chem. Eur. J.*, 2012, **18**, 15337-15344.

50. S. Wu, L. Chen, B. Yin and Y. Li, *Chem. Commun.*, 2015, **51**, 9884-9887.
51. S. Abednatanzi, P. G. Derakhshandeh, A. Abbasi, P. Van Der Voort and K. Leus, *ChemCatChem*, 2016, **8**, 3672-3679.
52. H. Fei, J. Shin, Y. S. Meng, M. Adelhardt, J. Sutter, K. Meyer and S. M. Cohen, *J. Am. Chem. Soc.*, 2014, **136**, 4965−4973.
53. X. Shu, Y. Yu, Y. Jiang, Y. Luan and D. Ramella, *Appl. Organometal. Chem.*, 2017, DOI: 10.1002/aoc.3862.
54. J. Hou, Y. Luan, J. Tang, A. M. Wensley, M. Yang and Y. Lu, *J. Mol. Catal. A: Chem.*, 2015, **407** 53-59.
55. A. Taher, D. W. Kim and I.-M. Lee, *RSC Adv.*, 2017, **7**, 17806-17812.
56. H. Liu, D. Ramella, P. Yu and Y. Luan, *RSC Adv.*, 2017, **7**, 22353-22359.
57. X. Du, Y. Luan, F. Yang, D. Ramella and X. Shu, *New. J. Chem.*, 2017, **41**, 4400-4405.
58. F. X. Llabres i Xamena, A. Abad, A. Corma and H. Garcia, *J. Catal.*, 2007, **250**, 294- 298.
59. A. Dhakshinamoorthy, M. Alvaro and H. Garcia, *ACS Catal.*, 2011, **1**, 48- 53.
60. B. R. Kim, J. S. Oh, J. Kim and C. Y. Lee, *Catal. Lett.*, 2016, **146**, 734-743.
61. Y. Qi, Y. Luan, J. Yu, X. Peng and G. Wang, *Chem. Eur. J.*, 2015, **21**, 1589−1597.
62. Z. Xue, J. Zhang, L. Peng, B. Han, T. Mu, J. Li and G. Yang, *ChemPhysChem*, 2014, **15**, 85-89.
63. X. Zhang, W. Dong, Y. Luan, M. Yang, L. Tan, Y. Guo, H. Gao, Y. Tang, R. Dang, J. Li and G. Wang, *J. Mater. Chem. A*, 2015, **3**, 4266-4273.
64. S. Aryanejad, G. Bagherzade and A. Farrokhi, *Inorg. Chem. Commun.*, 2017, **81**, 37-42.
65. A. Karmakar, L. M. D. R. S. Martins, S. Hazra, M. F. C. Guedes da Silva and A. J. L. Pombeiro, *Cryst. Growth Des.*, 2016, **16**, 1837−1849.
66. B. R. Kim, J. S. Oh, J. Kim and C. Y. Lee, *Bull. Korean Chem. Soc.*, 2015, **36**, 2799-2800.
67. S.-C. Chen, S.-N. Lu, F. Tian, N. Li, H.-Y. Qian, A.-J. Cui, M.-Y. He and Q. Chen, *Catal. Commun.*, 2017, **95** 6-11.
68. L. Peng, S. Wu, X. Yang, J. Hu, X. Fu, M. Li, L. Bai, Q. Huo and J. Guan, *New J. Chem.*, 2017, **41**, 2891-2894.
69. L. Peng, S. Wu, X. Yang, J. Hu, X. Fu, Q. Huo and J. Guan, *RSC Adv.*, 2016, **6**, 72433-72438.
70. J.-C. Wang, F.-W. Ding, J.-P. Ma, Q.-K. Liu, J.-Y. Cheng and Y.-B. Dong, *Inorg. Chem.*, 2015, **54**, 10865−10872.
71. A. Farrokhi, M. Jafarpour and R. Najafzade, *Catal. Lett.*, 2017, **147**, 1714-1721.
72. M. Lammert, M. T. Wharmby, S. Smolders, B. Bueken, A. Lieb, K. A. Lomachenko, D. De Vos and N. Stock, *Chem. Commun.*, 2015, **51**, 12578-12581.
73. T. W. Goh, C. Xiao, R. V. Maligal-Ganesh, X. Li and W. Huang, *Chem. Eng. Sci.*, 2015, **124**, 45-51.
74. S. Yuan, T.-F. Liu, D. Feng, J. Tian, K. Wang, J. Qin, Q. Zhang, Y.-P. Chen, M. Bosch, L. Zou, S. J. Teat, S. J. Dalgarno and H.-C. Zhou, *Chem. Sci.*, 2015, **6**, 3926-3930.
75. S. Abedi and A. Morsali, *ACS Catal.*, 2014, **4**, 1398-1403.
76. S. Proch, J. Herrmannsdorfer, R. Kempe, C. Kern, A. Jess, L. Seyfarth and J. Senker, *Chem. Eur. J.* , 2008, **14**, 8204 -8212.
77. H. Liu, Y. Liu, Y. Li, Z. Tang and H. Jiang, *J. Phys. Chem. C* 2010, **114**, 13362−13369.
78. J. Juan-Alcañiz, J. Ferrando-Soria, I. Luz, P. Serra-Crespo, E. Skupien, V. P. Santos, E. Pardo, F. X. Llabres i Xamena, F. Kapteijn and J. Gascon, *J. Catal.*, 2013, **307**, 295−304.
79. G. Chen, S. Wu, H. Liu, H. Jiang and Y. Li, *Green Chem.*, 2013, **15**, 230-235.
80. G.-J. Chen, J.-S. Wang, F.-Z. Jin, M.-Y. Liu, C.-W. Zhao, Y.-A. Li and Y.-B. Dong, *Inorg. Chem.*, 2016, **55**, 3058−3064.
81. Y. Goto, H. Sato, S. Shinkai and K. Sada, *J. Am. Chem. Soc.*, 2008, **130**, 14354-14355.
82. A. Taher, D.-J. Lee, B.-K. Lee and I.-M. Lee, *Synlett*, 2016, 1433-1437.
83. L. Peng, J. Zhang, Z. Xue, B. Han, X. Sang, C. Liu and G. Yang, *Nat. Commun.*, 2014, **5**, 4465.
84. A. Erxleben, *Coord. Chem. Rev.*, 2003, **246**, 203-228.
85. J. Taghavimoghaddam, G. P. Knowles and A. L. Chaffee, *Top. Catal.*, 2012, **55**, 571-579.
86. A. Aktas, I. Acar, E. T. Saka and Z. Biyiklioglu, *J. Organomet. Chem.*, 2016, **815-816**, 1-7.
87. S. R. Cicco, M. Latronico, P. Mastrorilli, G. P. Suranna and C. F. Nobile, *J. Mol. Catal. A: Chem.*, 2001, **165**, 135-140.
88. K. J. Gagnon, H. P. Perry and A. Clearfeld, *Chem. Rev.*, 2012, **112**, 1034-1054.
89. Y. P. Zhu, T. Y. Ma, Y. L. Liu, T. Z. Ren and Z. Y. Yuan, *Inorg. Chem. Front.*, 2014, **1**, 360-383.
90. N. C. Burtch, H. Jasuja and K. S. Walton, *Chem. Rev.*, 2014, **114**, 10575-10612.
91. G. K. H. Shimizu, R. Vaidhyanathan and J. M. Taylor, *Chem. Soc. Rev.*, 2009, **38**, 1430-1449.
92. M. T. Wharmby and P. A. Wright, *In Metal phosphonate chemistry: from synthesis to applications. Clearfeld A, Demadis K (eds) The Royal Society of Chemistry, London, pp. 317-343*, 2011.
93. A. Dhakshinamoorthy, A. M. Asiri and H. Garcia, *Angew. Chem., Int. Ed.*, 2016, **55**, 5414-5445.
94. X. Deng, Z. Li and H. Garcia, *Chem. - Eur. J.*, 2017, **23**, 11189-11209.
95. Y. Chen, H. J. Zheng, Z. Guo, C. M. Zhou, C. Wang, A. Borgna and Y. H. Yang, *J. Catal.*, 2011, **283**, 34.